



# Parallel Session 1

---

$e^+e^-$  Physics at  $Z^0$



**Organiser**

---

A. Donnachie (*Manchester*)

# Measurement of Electroweak Parameters from Z Decays into Fermion Pairs with the ALEPH detector at LEP

The ALEPH Collaboration

John Renner Hansen  
The Niels Bohr Institute  
Copenhagen.

## Abstract

This paper summarizes the results from the ALEPH analysis of the Z-resonance line shape and from the observation of asymmetries in the angular distributions of the  $q\bar{q}$  pairs from the Z decays.

## 1 Introduction.

This analysis of the Z-physics uses identified decays of the types  $Z \rightarrow q\bar{q}$  and  $Z \rightarrow l^+l^-$ . It is based on the full data sample recorded by the ALEPH detector until the end of June 1990. An integrated luminosity of  $3.8 \text{ pb}^{-1}$  were collected, corresponding to roughly 84,000 hadronic and 9,500 leptonic Z-decays. A detailed record on how the events are selected in the off-line data analysis have recently been published [1].

## 2 Z-resonance line shape.

From the energy scan over the region of the Z-resonance we have obtained cross-sections as a function of the center of mass energy for the five processes:  $Z \rightarrow q\bar{q}$ ,  $e^+e^-$ ,  $\mu^+\mu^-$ ,  $\tau^+\tau^-$  and  $l^+l^-$ , where  $l^+l^-$  represents any charged lepton pair. The five distributions are shown in figure 1 and 2 a-d. The normalization of the cross-sections are done by recording Bhabha events ( $e^+e^- \rightarrow e^+e^-$ ) simultaneous to the recording of Z decays. Only Bhabha events at small scattering angles were used, in the region where the theoretical calculations are most reliable. A detailed discussion of the luminosity measurement in ALEPH will be presented in a forthcoming publication [2]. An overall systematic error from the luminosity measurement is estimated to 1.3 %, including both the experimental error, 1.1%, and a theoretical error of 0.7%.

The effect of initial state radiation is included by convoluting the expression of the cross section with a suitable radiator function [3]. This effect is of the order of 30% at the peak, but is known to better than 0.5% [4]. The peak cross section due to Z exchange, when unfolded from initial state radiation, is:

$$\sigma_{f\bar{f}}^0 = \frac{12\pi}{M_Z^2} \frac{\Gamma_{ee}\Gamma_{f\bar{f}}}{\Gamma_Z^2} \quad (1)$$

$\Gamma_{ee}$  and  $\Gamma_{f\bar{f}}$  are the partial widths of Z decay into  $e^+e^-$  and into any fermion pair  $f\bar{f}$  respectively,  $\Gamma_Z$  is the total width and  $M_Z$  the mass of the Z boson. In the various fits that have been performed, the interference term has been parametrized assuming the Standard Model.

Fitting the hadronic and three lepton pair cross sections simultaneously, one can determine six parameters: the Z mass, the full width, the peak hadronic cross section ( $\sigma_{\text{had}}^0$ ) and the three lepton partial widths in units of the hadronic width. The fit results for the six parameters are:

$$M_Z = (91.189 \pm 0.013_{\text{exp}} \pm 0.030_{\text{LEP}}) \text{ GeV}$$

$$\Gamma_Z = (2.502 \pm 0.025) \text{ GeV}$$

$$\sigma_{\text{had}}^0 = (41.74 \pm 0.63) \text{ nb}$$

$$\Gamma_{\text{had}}/\Gamma_{ee} = (20.62 \pm 0.55)$$

$$\Gamma_{\text{had}}/\Gamma_{\mu\mu} = (21.55 \pm 0.47)$$

$$\Gamma_{\text{had}}/\Gamma_{\tau\tau} = (21.24 \pm 0.47);$$

The  $\chi^2$  is 44 for 52 degrees of freedom.

Assuming lepton universality we repeat the fit for four parameters,  $M_Z$ ,  $\sigma_{\text{had}}^0$ ,  $\Gamma_Z$ ,  $\Gamma_{l^+l^-}/\Gamma_{\text{had}}$  using the hadron sample and the lepton sample selected without distinguishing the final state lepton flavour (see Figure 2-d).  $\Gamma_{l^+l^-}$  is defined as 1/3 of  $\Gamma_{\text{leptons}}$ .

The result is:

$$M_Z = (91.185 \pm 0.013_{\text{exp}} \pm 0.030_{\text{LEP}}) \text{ GeV}$$

$$\Gamma_Z = (2.505 \pm 0.026) \text{ GeV}$$

$$\sigma_{\text{had}}^0 = (41.91 \pm 0.63) \text{ nb}$$

$$\Gamma_{\text{had}}/\Gamma_{l^+l^-} = (20.96 \pm 0.31)$$

with  $\chi^2=16.4$  for 22 degrees of freedom. The result of the fit is shown in figures 1 and 2.

Figure 1: Cross section for  $e^+e^- \rightarrow \text{hadrons}$  as a function of the centre-of-mass energy together with the result of the fit.

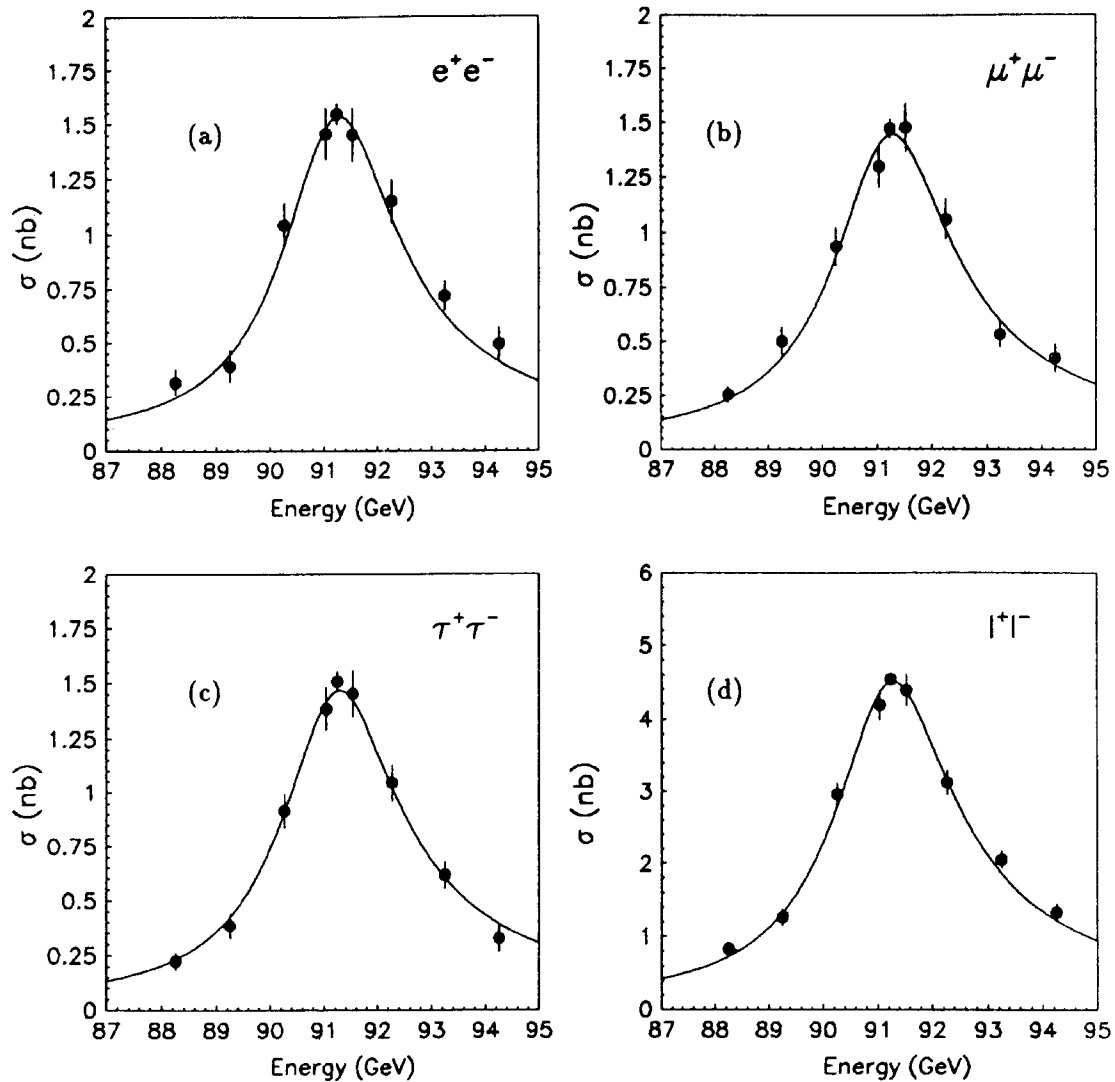
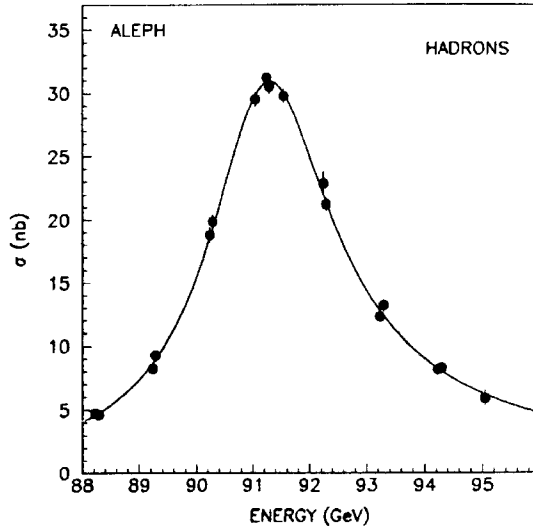


Figure 2 : Cross sections for  $e^+e^- \rightarrow \text{lepton pairs}$  as a function of the centre-of-mass energy. For points where the energy difference is less than 100 MeV the average cross section is plotted. The full line is result of the fit.

Equivalently the results can be expressed by  $\Gamma_{l+l-}$  and  $\Gamma_{\text{inv}}/\Gamma_{l+l-}$  rather than by  $\sigma_{\text{had}}^0$  and  $\Gamma_Z$  where the invisible width is

$$\Gamma_{\text{inv}} = \Gamma_Z - \Gamma_{\text{had}} - \Gamma_{ee} - \Gamma_{\mu\mu} - \Gamma_{\tau\tau}$$

$$\Gamma_{l+l-} = (84.3 \pm 1.1) \text{ MeV}$$

$$\Gamma_{\text{inv}}/\Gamma_{l+l-} = 5.75 \pm 0.25$$

The number of light neutrino species can be obtained from the measured cross sections assuming  $\Gamma_{\text{inv}} = N_\nu \Gamma_\nu$ . With

$$\Gamma_Z = \Gamma_{\text{had}} + 3\Gamma_{l+l-} + N_\nu \Gamma_\nu, \quad (2)$$

$$N_\nu = \frac{\Gamma_{l+l-}}{\Gamma_\nu} \left( \sqrt{\frac{12\pi}{M_Z^2 \sigma_{\text{had}}^0}} R - R - 3 \right), \quad (3)$$

where  $R = \Gamma_{\text{had}}/\Gamma_{l+l-}$ .

Using the standard model prediction for  $\Gamma_{l+l-}/\Gamma_\nu = 0.5010 \pm 0.0005$  and  $R = 20.93 \pm 0.21$  [5] and our measured values of  $M_Z$  and  $\sigma_{\text{had}}^0$  one finds:

$$N_\nu = 2.89 \pm 0.12_{\text{exp}} \pm 0.03_{\text{theory}}.$$

The second error comes from the uncertainty in the prediction of  $R$  which is dominated by the uncertainty in the QCD correction. By using our measured value of  $R = 20.96 \pm 0.31$ , we obtain:

$$N_\nu = 2.88 \pm 0.12.$$

The importance of this last result compared to the previous one, is that here the only assumption is the ratio  $\Gamma_{l+l-}/\Gamma_\nu$ . This result is still valid if unexpected states yielding hadrons are present in the  $Z$  decay. From the measurement of  $\Gamma_{l+l-}$  the value of  $\sin^2 \theta_W^f(M_Z^2)$  is found to be:

$$\sin^2 \theta_W^f(M_Z^2) = 0.2294 \pm 0.0036$$

### 3 $q\bar{q}$ charge asymmetry.

A forward-backward asymmetry near the  $Z$  pole arises from the difference between left-handed and right-handed coupling to the  $Z$ , both for the initial state  $e^+e^-$  pair and for the final state quarks. The asymmetry can for a flavour  $f$  be written as:

$$A_{FB}^f = \frac{\sigma_F^f - \sigma_B^f}{\sigma_F^f + \sigma_B^f} \quad (4)$$

$\sigma_F^f$  is the cross-section for emitting the fermion from a  $Z$ -decay in the same direction as the incoming electron.  $\sigma_B^f$  is the cross-section for fermion emission in the opposite direction. For massless quarks of flavour  $f$  the asymmetry factor can be written as

$$A_{FB}^f = \frac{\cos \Theta_{max}}{(1 + \cos^2 \Theta_{max})/3} A_e A_f \quad (5)$$

where  $\Theta_{max}$  is the maximum polar angle, set by the acceptance of the experiment.  $A_e$  and  $A_f$  are the left-right asymmetry in the neutral current coupling of the electron and the quark respectively. For any fermion,  $A_f$  is given by:

$$A_f = \frac{2g_v^f g_a^f}{(g_v^f)^2 + (g_a^f)^2} \quad (6)$$

where  $g_v^f$  and  $g_a^f$  are the vector and axial-vector coupling of fermion  $f$ .

As the quarks are not observed directly, we use the charge of the final state hadrons as a measure of the original charge. This is typically done by calculating the weighted sum over the observed charge. In ALEPH the event thrust axis is constructed, with the positive direction defined as the one pointing into the hemispheres of ALEPH with positive  $z$ -coordinates. The weighted charge of all hadrons with their momentum vectors pointing into the positive thrust direction (Forward) is given by:

$$Q_F = \frac{\sum_{\vec{p}_i \cdot \vec{e}_T > 0} |\vec{p}_i \cdot \vec{e}_T|^\kappa \cdot q_i}{\sum_{\vec{p}_i \cdot \vec{e}_T > 0} |\vec{p}_i \cdot \vec{e}_T|^\kappa} \quad (7)$$

$\kappa$  is a free parameter which allows a study of the sensitivity and the systematic error of this method. In the following the results are presented for  $\kappa = 1.0$ .  $Q_B$  defines the weighted charge sum over the particles observed in the opposite thrust hemisphere. The charge difference,  $Q_{FB} = Q_F - Q_B$ , and the total charge  $Q = Q_F + Q_B$  of the event is in the ideal case, at the quark level, two times the quark charge ( $2q_f^0$ ) and 0 respectively.  $q_f$  is in the following defined as the observed charge difference from flavour  $f$ . In a Monte Carlo simulation we find  $q_u = 0.430$ ,  $q_d = -0.214$ ,  $q_s = -0.298$ ,  $q_c = 0.174$  and  $q_b = -0.215$ . The numerical value of  $q_f$  is always smaller than  $2 \cdot |q_f^0|$ . The relation between  $\langle Q_{FB} \rangle$ ,  $A_e$  and  $A_q$  can be expressed as:

$$\langle Q_{FB} \rangle = \frac{\cos \Theta_{max}}{(1 + \cos^2 \Theta_{max})/3} A_e \sum_{f=1}^5 q_f A_f \frac{\Gamma_f}{\Gamma_{Had}} \quad (8)$$

$$\Gamma_f = C \cdot ((g_v^f)^2 + (g_a^f)^2) \quad (9)$$

Combined with eq. 6 one finds

$$\langle Q_{FB} \rangle = A_e \cdot C' \cdot \sum_{f=1}^5 q_f \cdot g_v^f \cdot g_a^f \quad (10)$$

By the method described above we measure the average charge difference:

$$\langle Q_{FB} \rangle = -0.00107 \pm 0.0021_{\text{stat}} \pm 0.0010_{\text{sys}}$$

and the average total charge:

$$\langle Q \rangle = -0.0001 \pm 0.0018_{\text{stat}} \pm 0.0010_{\text{sys}}$$

While the total charge vanishes on average, there is a significant forward-backward asymmetry in the reconstructed charge. The systematic error comes from possible charge *and* forward-backward asymmetric effects in track finding and reconstruction.

The coupling constants in eq. 10 can be expressed in terms of  $\sin^2\theta_W^Z(M_Z^2)$  yielding:

$$\sin^2\theta_W^Z(M_Z^2) = 0.225 \pm 0.005_{stat} \pm 0.002_{exp-sys} \pm 0.004_{th-sys}$$

The theoretical error comes from uncertainties in calculating the observed charges  $q_f$  and were obtained by varying the parameters of the LUND monte-carlo by conservative amounts.

One can also use the couplings of quarks as measured in neutrino scattering [6], and extract the electron couplings in a more model-independent way:

$$A_e = \frac{2 \cdot g_v^e \cdot g_a^e}{(g_v^e)^2 + (g_a^e)^2} = 0.172 \pm 0.059$$

or

$$\frac{g_v^e}{g_a^e} = 0.090 \pm 0.0031$$

This result establishes that the sign of  $g_v^e$  and  $g_a^e$  are the same.

## 4 Conclusion

The analysis of the ALEPH data has provided a new very precise measurement of some of the standard model parameters. The observation of an asymmetry in the charge distribution in final state  $q\bar{q}$  events has provided a new measurement of the ratio of the vector to the axial-vector coupling constant of the electron. Apart from giving the actual ratio it has also provided the relative sign of the two coupling constants. The errors on this measurement shows that the method, in the future with high statistic, will give a precise measurement of the electro-weak coupling constants.

## References

- [1] D. Decamp *et al.* (ALEPH Collaboration). Measurement of the electroweak parameters from Z decays into fermion pairs. CERN Preprint EP/90-104. Submitted to *Zeitschrift für Physik C*
- [2] A detailed discussion of the measurement of the luminosity in the ALEPH detector will soon be published in *Zeitschrift für Physik C*
- [3] E.A. Kuraev, V.S. Fadin. Sov.J.Nucl.Phys. 41(1985)466, G.Altarelli, G.Martinelli, in "Physics at LEP" CERN 86-02 (1986) Vol. I,47, O.Nicosini, L.Trentadue Phys. Lett. B196(1987)551.
- [4] F.A. Berends *et al.* Z Line Shape group in "Proceedings of the Workshop of Z Physics at LEP" CERN Report 89-08 Vol.I,89.
- [5] This value of R and its error are obtained as the prediction of the Standard Model [4] for  $\alpha_s = 0$  multiplied by the QCD correction computed in G.D'Agostini, W.deBoer and G.Grindhammer. Phys. Lett. B229(1989)160.
- [6] Amaldi *et al.* Comprehensive analysis of data pertaining to the weak neutral current and the intermediate-vector-boson masses. Phys. Rev. D36 (1987) 1385.

ASYMMETRIES AND POLARIZATION IN THE Z BOSON  
DECAYS TO LEPTON PAIRS  
ALEPH Collaboration

J.C. BRIENT

Laboratoire de Physique Nucléaire et des Hautes Energies  
Ecole Polytechnique, IN2P3-CNRS  
F-91128 Palaiseau CEDEX, France

Abstract

The ALEPH results concerning the charge forward backward asymmetries of the leptons in the decays of the Z boson are presented. Three different decay channels of the  $\tau$  have been used to measure the polarization. A first value of the vector coupling  $g_V^\tau$  of the  $\tau$  lepton is derived from that measurement. Finally, the different values obtained by the ALEPH collaboration for the electroweak parameters of the leptons are summarized, leading to a  $\sin^2\theta_W = 0.2283 \pm 0.0027$ .

## 1. Introduction

The data collected by ALEPH in 1989 and part of 1990 are used to extract the charge forward backward asymmetries ( $A_{FB}$ ) in the reaction  $e^+e^- \rightarrow Z \rightarrow e^+e^-$ ,  $\mu^+\mu^-$  and  $\tau^+\tau^-$ . The measurement of  $A_{FB}$  as a function of  $\sqrt{s}$  leads to the ratio of the vector coupling ( $g_{Vl}$ ) to the axial coupling ( $g_{Al}$ ) of the lepton. Using the constraint of the partial width of the Z into leptons, we obtain  $g_{Vl}$  and  $g_{Al}$ . In the  $\tau^+\tau^-$  channel, the  $\tau$  polarization has been measured using three different  $\tau$  decay channels. Combining this result with the partial width  $\Gamma(Z \rightarrow \tau^+\tau^-)$  presented by ALEPH in this conference [1], we obtain the first measurement of  $g_{V\tau}$ , the vector coupling of the  $\tau$ . All the different values of  $g_{Vl}$  and  $g_{Al}$  obtained by ALEPH are summarized, and combined values computed. In the framework of the Standard Model, we deduce  $\sin^2\theta_W$  from partial widths on one side and from the  $A_{FB}$  and  $\tau$  polarization on the other side. The two values are in good agreement and the combined value is calculated and used to give a limit on the top quark mass.

## 2. Lepton Asymmetries

The selection procedures for each individual channel are described elsewhere in these proceedings [1]. In the case of the Z decay to  $\tau^+\tau^-$ , an additional selection is needed to reject all possible t-channel  $e^+e^-$  contribution, which could bias the  $A_{FB}$  measurement. This additional selection is based on the tagging of at least one track with an energy deposited in the first 4 radiation length (X0) of the electromagnetic calorimeter (ECAL) compatible with a minimum ionizing particle track. To extract the value of  $A_{FB}$  at each beam energy, a maximum likelihood is performed on the polar angle distribution of the lepton  $l^-$  (In the case of  $e^+e^-$  final state, the t-channel contribution, calculated using the formulae of Greco [4] is first subtracted from the data distribution).

Assuming lepton universality, a global fit of the axial and vector couplings of the leptons is performed on the asymmetries as a function of  $\sqrt{s}$  [2]. Figure 1 shows the asymmetries for the three different channels. The points in black are used in the fit, (white points in  $e^+e^-$  final state, far from the Z peak, are too sensitive to t-channel subtraction), while the curve is the result of the fit. The ratio  $g_{Vl} / g_{Al}$  is measured to be :

$$\frac{g_{Vl}}{g_{Al}} = 0.090^{+0.024}_{-0.019}$$

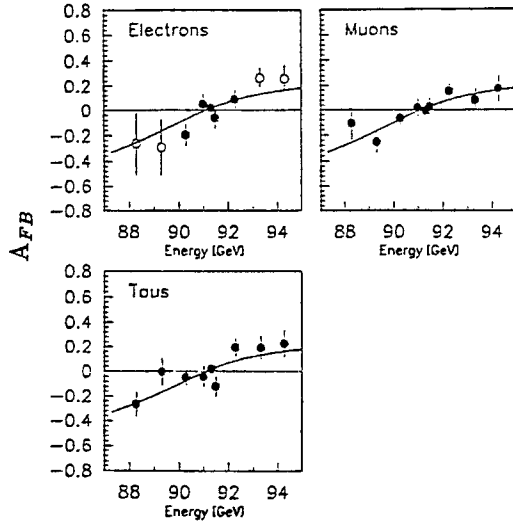


figure 1.

Charge forward backward asymmetry for each of the three leptons as a function of  $\sqrt{s}$

### 3. $\tau$ polarization

The mean value of the  $\tau$  polarization averaged over the polar angle, is related to  $g_V / g_A$ . Three  $\tau$  decay channel have been used to measure it,  $\tau \rightarrow \pi \nu_\tau$ ,  $\tau \rightarrow a_1 \nu_\tau$  (with  $a_1$  decays to  $3\pi^\pm$ ) and  $\tau \rightarrow \mu \nu_\mu \nu_\tau$ .

#### 3.1 $\pi \nu_\tau$ channel

For the  $\pi$  channel, the relevant variable to measure the polarization is the ratio  $x = E_\pi / E_\tau$  (where  $E_\pi$  ( $E_\tau$ ) is the  $\pi^\pm$  ( $\tau^\pm$ ) energy). In fact, the  $\tau$  energy is approximated by the beam energy and radiative corrections are taken into account in the fit, using the Monte Carlo. The  $\pi$  channel is distinguished from the other  $\tau$  decays by using the ECAL (to reject  $\pi^\pm + \pi^0$ 's and  $e^\pm$  channel of the  $\tau$  decays) and the Hadron Calorimeter (HCAL) (to reject the  $\mu$  channel). The different sources of background have been carefully studied. Uncertainties on this background will be taken into account in the systematic errors quoted in the result. Figure 2 shows the  $dN / dx$  distribution (raw data in dashed histogram corresponding to a sample of 470 events).

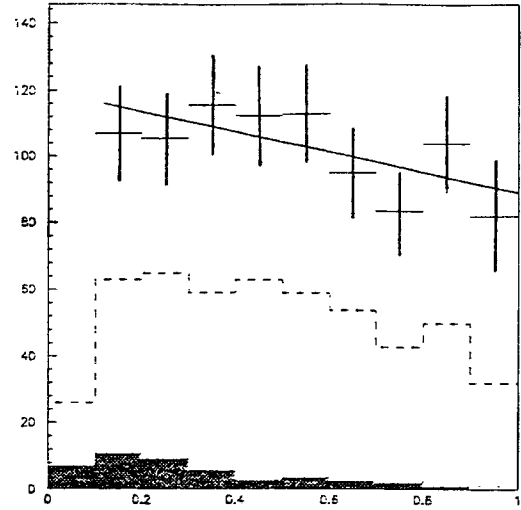


figure 2.

$dN/dx$  distribution for the  $\tau \rightarrow \pi \nu_\tau$  sample

The contribution of the other  $\tau$  decays in the selected  $\pi$  sample (black histogram) is calculated from Monte Carlo, with full simulation of the detector. Comparison between test beam data and Monte Carlo allows a check of the computed efficiency as a function of the pion energy. After subtraction of the other  $\tau$  decay contributions and correction for efficiency, the spectrum is shown as points with error bars. The result of the fit of the polarization is the straight line superimposed on the figure. The fit gives the following value:

$$P_\tau = -0.144 \pm 0.09 \text{ (stat.)} \pm 0.058 \text{ (syst.)}$$

#### 3.2 $\mu \nu_\mu \nu_\tau$ channel

To select this channel, a low energy deposition in the ECAL is first required. After this crude selection, the background from other  $\tau$  decays is entirely coming from the  $\pi^\pm$  channel, when the charged pion does not interact in the ECAL. To obtain a clean sample of  $\mu$ , the penetration of the track and the shower width in HCAL are used to identify the muon. In addition, to reject the possible  $Z \rightarrow \mu^+ \mu^-$  and  $\gamma\gamma \rightarrow \mu^+ \mu^-$  background, kinematical cuts are applied and events with muons identified on both

hemispheres are rejected. The  $\pi^\pm$  contamination in our sample is obtained from the study of  $\tau$  decays containing  $\pi^0$ . Finally, using the muon-chambers, the  $\mu$  identification efficiency as a function of  $E_\mu$  is measured directly from the data. The sample after background subtraction contains 654 events.

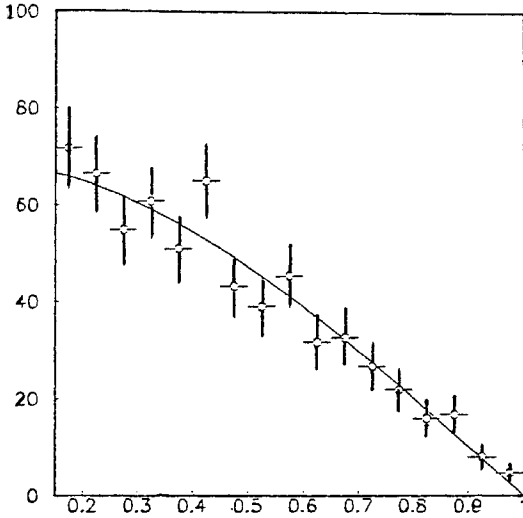


figure 3.

$dN/dx$  distribution for the  $\tau \rightarrow \mu\nu_\mu\nu_\tau$  sample.

Here again the relevant variable is the muon energy normalized to the tau energy ( $x$ ), and the  $dN/dx$  distribution for the  $\tau \rightarrow \mu\nu_\mu\nu_\tau$  channel is shown in figure 3, where the curve is the result of the fit :

$$P_\tau = -0.184 \pm 0.186 \text{ (stat.)} \pm 0.045 \text{ (syst.)}$$

### 3.3 $a_1 \nu_\tau$ channel

To select this channel, we first required to have 3 good quality tracks [2] in one hemisphere. The ECAL and the TPC  $dE/dx$  information are used to tag the electron track, and 3 prong candidates are rejected if one of them is consistent with an electron (in order to reject  $\pi^\pm + \pi^0$ 's with photon conversion). The residual background at this level is the  $\tau$  decay to  $3\pi^\pm + \pi^0$ 's. To reject this kind of events, the good granularity of the ECAL is used, tagging photons from  $\pi^0$  decays in the first 4X0 of the

ECAL. Finally, events with at least one entry in the  $\rho$  mass band in the Dalitz plot of  $(\pi^+\pi^-)$  squared mass, are selected. The measure of the polarization in this channel uses two angles [3]:  $\theta$  is the angle between the  $3\pi^\pm$  direction and the  $\tau$  laboratory line of flight in the  $\tau$  rest frame and  $\psi$  is the angle between the direction of the normal to the plane defined by the pions momenta and the 3 pions laboratory line of flight in the 3 pions rest frame.

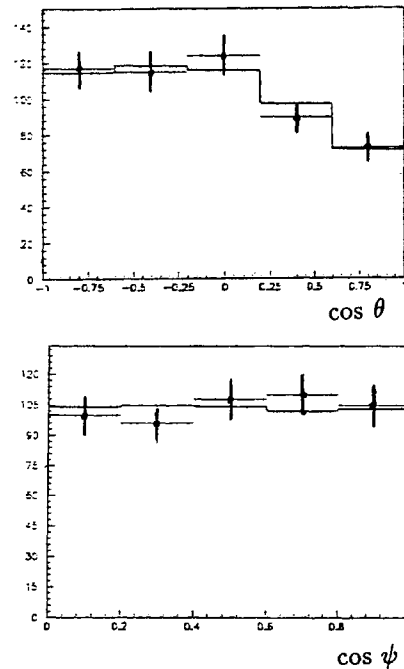


figure 4.

$\cos \theta$  and  $\cos \psi$  distribution for the  $\tau \rightarrow a_1 \nu_\tau$  sample

Figure 4 shows the experimental distributions (points with error bars) and the result of the fit (in histogram), where the Monte Carlo is used to give the expected distribution for each helicity.

$$P_\tau = -0.13 \pm 0.24 \text{ (stat.)} \pm 0.08 \text{ (syst.)}$$

### 3.4 Conclusion on $\tau$ polarization

The  $\tau$  polarization in the Z decays to  $\tau^+\tau^-$



has been measured, using three different  $\tau$  decays channel. There is an agreement between the three measures and the combined value is  $-0.151 \pm 0.087$ . This leads to the ratio of the vector to axial coupling of the  $\tau$  :  $(g_V/g_A)\tau = 0.076 \pm 0.044$ . Using the partial width  $\Gamma(Z \rightarrow \tau^+ \tau^-)$ , we obtain the first measurement of the vector coupling of the  $\tau$ :

$$g_{V\tau} = -0.037 \pm 0.023$$

and

$$g_{A\tau} = -0.494 \pm 0.008$$

#### 4. Electroweak parameters of the Standard Model

Table 1 summarizes the results obtained from the  $A_{FB}$  of the leptons, the  $A_{FB}$  of the  $q\bar{q}$  [1], and from the  $\tau$  polarization.

Input	$g_V/g_A$ lepton	$\sin^2 \theta_W$
$\tau$ pol.	$0.076 \pm 0.044$	$0.2311 \pm 0.011$
$A_{FB}$ lept.	$0.090^{+0.024}_{-0.019}$	$0.2275^{+0.0059}_{-0.0047}$
$A_{FB}$ $q\bar{q}$	$0.090 \pm 0.031$	$0.225 \pm 0.0067$
combi.	$0.088 \pm 0.016$	$0.2271^{+0.0041}_{-0.0036}$

Table 1.

From the  $A_{FB}$  and  $\tau$  polarization in ALEPH, ratio of the vector to axial coupling of the leptons and  $\sin^2 \theta_W$  in the framework of the standard model.

To measure the  $g_{Vl}/g_{Al}$  of the electron, in the  $A_{FB}$  of  $q\bar{q}$ , we assume quark family universality and use low energy neutrino data for the values of the quark vector and axial couplings. This is not needed for the measurement of  $\sin^2 \theta_W$ , since, in

the framework of the standard model, the quark couplings are only dependent on this parameter.

The combined value of  $\sin^2 \theta_W$  in table 1, is in agreement with the value extracted from the lepton partial widths :  $0.2294 \pm 0.0037$ . Combining these two measures leads to :

$$\sin^2 \theta_W(M_Z^2) = 0.2283 \pm 0.0027$$

A global fit of  $g_{Vl}$  and  $g_{Al}$  has been performed using all  $A_{FB}$ , the lepton partial widths and  $\tau$  polarization. The fit gives the following values for the vector and axial coupling of the leptons:

$$g_{Vl} = -0.0442^{+0.009}_{-0.008}$$

$$g_{Al} = -0.5019 \pm 0.0034$$

In the fit the sign of  $g_{Al}$  is assumed negative. The contours at 68% and 99% of confidence level in the plane  $g_{Vl}$ ,  $g_{Al}$  are shown in figure 5.

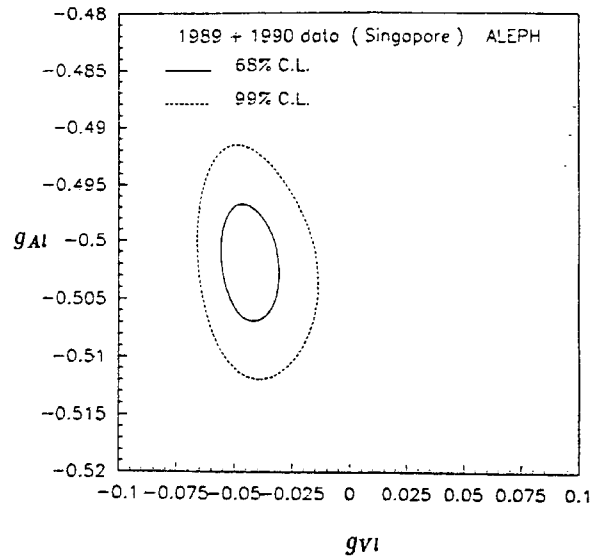


figure 5.

68% and 99% confidence level contours, in the plane  $g_{Vl}$   $g_{Al}$ , from the global fit including  $A_{FB}$ , lepton partial widths and  $\tau$  polarization.

Using the mass of the Z boson measured in ALEPH [1], the  $\sin^2 \theta_W$  presented here,

and the ratio  $M_W/M_Z$  [5] measured in  $p\bar{p}$  collider and from neutrino experiments [6], we can extract a limit for the top quark mass, through the radiative corrections. Figure 6 shows the 68% confidence level region from these different inputs. The overlap region corresponds to the following value :

$$M_{top} = 140 \pm 35 \pm 3_{M_Z} \pm 1_{\alpha_s} \pm 20_{M_{Higgs}} \text{ GeV}$$

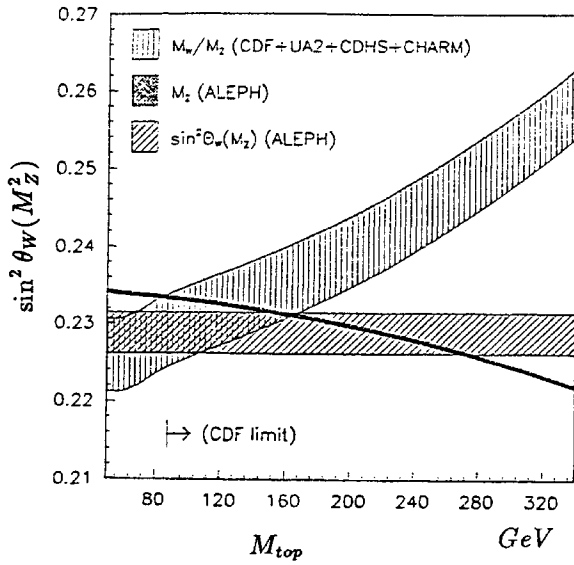


figure 6.

$\sin^2 \theta_W (M_Z^2)$  variation as a function of the top quark mass

## 5. Conclusion

From the data collected by ALEPH in 1989 and part of the 1990 period, the charge forward backward asymmetries of the leptons have been measured and used to determine the ratio of vector to axial couplings of the leptons,  $g_{VI} / g_{AI} = 0.090^{+0.024}_{-0.019}$ . The polarization of the  $\tau$ , together with the partial width  $\Gamma(Z \rightarrow \tau^+ \tau^-)$ , allows a first measurement of the vector coupling of the  $\tau$ ,  $g_{V\tau} = -0.037 \pm 0.023$ . Using the  $A_{FB}$  of the leptons, the  $A_{FB}$  of the  $q\bar{q}$ , the partial widths of the Z to leptons, and the

$\tau$  polarization, the vector and axial weak couplings of the leptons,  $g_{VI} = -0.0442 \pm 0.009$  and  $g_{AI} = -0.5019 \pm 0.0034$ , have been determined. Finally, in the framework of the standard model, the values of  $\sin^2 \theta_W$ , extracted from the different measurements, are in agreement. The combined value,  $\sin^2 \theta_W = 0.2283 \pm 0.0027$ , agrees well with previous measurement ([2] and references cited therein)

## References

- [1] J.R. Hansen, ALEPH Collaboration, this proceeding
- [2] D. Decamp et al., *CERN-PPE/90-104, Submitted to Z-Physik, 1990*
- [3] A. Rouge, *Z. Phys C48 (1990) 75*
- [4] M. Greco, *Phys.Lett. B177(1986) 97 and Riv.Nuovo Cimento 11(1988) 1*
- [5] J. Alitti et al, (UA2 Collaboration) *Phys. Lett. B241 (1990)150*  
P. Shalbach (CDF Collaboration) *APS conf., Washington DC, april 1990*
- [6] H. Abramowicz et al, (CDHS Coll.) *Phys. Lett. 57(1986) 298*  
A. Blondel et al, *Z. Phys. C45 (1990) 361*  
J.V. Allaby et al, (CHARM Coll.) *Phys. Lett. B177 (1986) 446*  
and *Z. Phys. C36 (1987) 611*

# AN OVERVIEW OF DELPHI AND ITS RESULTS

UGO AMALDI  
CERN, Geneva, Switzerland

## ABSTRACT

A short description of the DELPHI detector and of its performances is followed by two sections devoted to the results on the Z-line shape obtained with 68,000 hadronic events collected in the first year of data taking at LEP. The last sections summarise a number of other results obtained in many different areas: particle searches, multiplicity distributions, QCD, heavy flavour decays.

### 1. The DELPHI detector.

A detailed description of the DELPHI detector, of the triggering conditions and of the analysis chain can be found in [1]. The charged tracks are measured in the 1.2 Tesla magnetic field by a set of four cylindrical tracking detectors: the Microvertex Detector (MD) which has layers at 9 cm and 11 cm from the vertex, the Inner Detector (ID) covering radii 12 to 28 cm, the Time Projection Chamber (TPC) from 30 to 122 cm, and the Outer Detector (OD) between 197 and 208 cm. The end caps are covered by the Forward Chambers A and B, at polar angles  $10^\circ$  to  $36^\circ$  on each side. A layer of Time-of-Flight (TOF) counters is installed beyond the magnet coil for triggering purposes. The 1.1 m thick Hadron Calorimeter is followed, both in the barrel and forward, by two or three layers of Muon Chambers.

The electromagnetic energy is measured by the High Density Projection Chamber (HPC), and by the Forward Electromagnetic Calorimeter (FEMC) in the end caps. The HPC is a high granularity gaseous calorimeter covering polar angles  $40^\circ$  to  $140^\circ$ . It is mounted inside the cryostat of the Superconducting Coil, which has a diameter of 5.2 m. The FEMC consists of  $2 \times 4500$  lead glass blocks (granularity  $1 \times 1$  degrees), covering polar angles from  $10^\circ$  to  $36^\circ$  on each side.

Two novel detectors are used to 'flavour tag' the events, one of the main aims of DELPHI, a Detector with Lepton, Photon and Hadron Identification. The two layers of the microvertex sili-

con detector contain  $\sim 50,000$  channels. At present the measurement accuracy in the  $r\varphi$  plane is  $7 \mu\text{m}$  and the alignment error is  $\sim 15 \mu\text{m}$  for the external layer (at 11 cm from the vertex) and  $\sim 10 \mu\text{m}$  on the internal layer (at 9 cm from the vertex). In 1991 a new beryllium pipe of smaller diameter will allow the installation of an inner layer at  $\sim 6$  cm from the vertex. The second novel detector is the Barrel RICH, which is described in [1]. Charged particles emit ultraviolet photons in a liquid radiator ( $C_6F_{14}$ ) and in a gas radiator ( $C_5F_{12}$ ). During the first months of running half of the liquid radiators were installed. Fig. 1 shows the rings due to muons coming from Z-decays. The number of photons per track is 10, in good agreement with the Monte Carlo prediction [12]. When the temperature of the BRICH will be raised to  $\sim 40^\circ\text{C}$ , the absorption of the ultraviolet photons in the detector drift volumes will increase by  $\sim 20\%$ . At the beginning of 1991 all the liquid radiators and the final gas will be introduced and the BRICH will be fully operational.

### 2. Hadronic and leptonic decays of the Z-boson.

The results summarised in this and the following section are described in more detail in a paper submitted to this Conference [2]. They are based on approximately 68,000 hadronic events and about 4,000 electron, muon and tau-lepton pairs recorded between Sept. 89 and July 90.

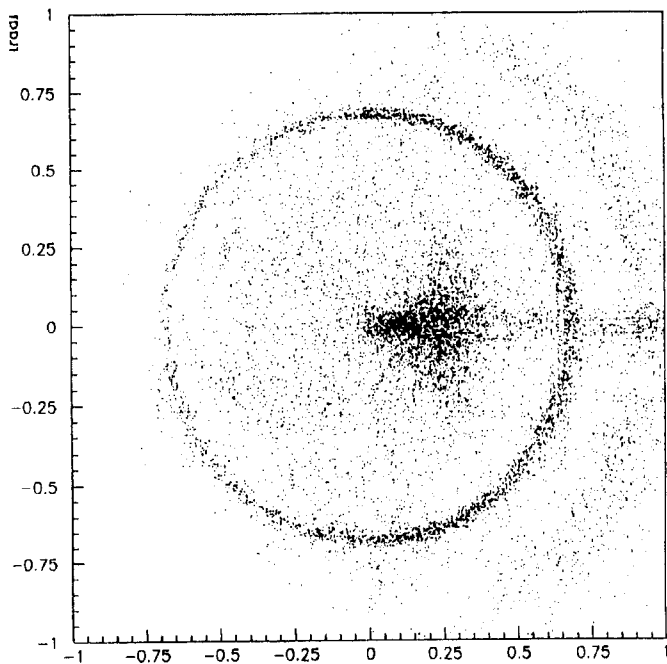


Figure 1 : Overlap of about 200 'liquid' rings due to muons from Z-decay. The spot at the center is due to the muons traversing the RICH detector.

The luminosity measurement has improved with respect to our previous publication [3] by the addition of a lead mask ("butterfly-wings") in front of one of the Small Angle Tagger (SAT) arms to cover a dead zone in the vertical plane. The overall systematic error on the 1990 luminosity measurement is  $1.7\%(\text{expt.}) \pm 1.0\%(\text{theory})$ .

The analysis of the 1990 data (about 58,000 hadronic events) is very similar to the one described in [3].

The hadronic event selection relies only on charged tracks measured in the barrel region. The track selection criteria are the same as for the 1989 data. The overall normalisation uncertainty for the 1989 data remains unchanged at 2.6%. For the 1990 data, the reduced systematic error on the luminosity measurement gives an overall normalisation uncertainty of 2.3% (i.e. 1.1% for the hadronic event selection and 2.0% for the luminosity).

For the *electron-positron channel* the present analysis follows closely the one described in [4] with some important improvements. In particular, the fiducial cuts (to avoid the border regions of the HPC modules) are better understood; the

tau pair background is reduced to  $2 \pm 1\%$ , the t-channel subtraction is made using the formulae of [5]. A total sample of 1389 events were selected, corresponding to an integrated luminosity of  $2.6 \text{ pb}^{-1}$ . The systematic error on the  $e^+e^-$  cross-section is estimated to be 1.6%, due to 0.1% from the trigger, 1.0% from the tau-lepton background subtraction, 0.8% for the selection efficiency and 1.0% for the t-channel subtraction.

The present analysis of the *muon-antimuon channel* has several significant changes from the one described in [4]. The main emphasis has been put on increasing the muon pair identification efficiency inside an "extended-barrel" region defined to lie in the polar angle range  $43^\circ < \theta < 137^\circ$ . A total sample of 1618 events were selected corresponding to an integrated luminosity of  $2.5 \text{ pb}^{-1}$ . The systematic error on the  $\mu^+\mu^-$  cross-section is (apart from the luminosity uncertainty) estimated to be 1.9%, due to 1.0% from the trigger, 1.35% from selection efficiency, 0.5% for particle identification, 1.0% from the tau-lepton background subtraction and 0.3% from the cosmic ray background. A 1.0% systematic error on the asymmetry is estimated from the number of like sign pairs and from the charge asymmetry in each hemisphere taken separately.

For the *tau-antitau channel* we follow very closely the analysis described in [4] but with a much better understanding of selection efficiencies and backgrounds. A total sample of 1016 events were selected corresponding to an integrated luminosity of  $2.3 \text{ pb}^{-1}$ . The systematic error on the  $\tau^+\tau^-$  cross-section is (apart from the luminosity uncertainty) estimated to be 2.7%, due to 1.0% from the trigger 1.5% from selection efficiency, and 2.0% from hadronic background subtraction and secondary interactions. A 1.0% systematic error on the asymmetry is estimated from the charge asymmetry in each hemisphere taken separately.

In this new analysis we have also selected the leptonic pair final states without distinguishing the leptonic flavor (*blind analysis*). The event selection depends only on the information from the TPC. A topology cut is applied to the selected events. The cuts are equivalent to requiring a two jet configuration with topology 1.vs.N ( $N=1,\dots,5$ ) and isolation angle of  $150^\circ$  between

the isolated track and the jet. The efficiency for detecting each type of charged lepton with these cuts has been calculated with a Monte Carlo simulation giving 95% for  $e^+e^-$ , 96% for  $\mu^+\mu^-$  and 84% for  $\tau^+\tau^-$ . A total sample of 3187 events were selected, for an integrated luminosity of  $1.9 \text{ pb}^{-1}$ . The systematic error on the flavour-blind lepton cross-section is (apart from the luminosity uncertainty) estimated to be 1.3%, due to 1.0% from the trigger, 0.5% from track selection efficiency and 0.6% from background subtraction.

### 3. Extraction of the Z-parameters.

The  $Z^0$  resonance parameters were determined by fitting the hadronic and leptonic data with the theoretical cross-sections computed in [6]. A 3 parameter fit gives (with  $\chi^2/d.o.f = 12.4/(17-3)$ )

$$\begin{aligned} M_Z &= 91.191 \pm 0.014(\text{stat}) \pm 0.030(\text{syst})\text{GeV}/c^2 \\ \Gamma_Z &= 2.466 \pm 0.027(\text{stat}) \pm 0.010(\text{syst})\text{GeV}/c^2 \\ \sigma_0 &= 42.38 \pm 0.30(\text{stat}) \pm 0.97(\text{syst})\text{nb}. \end{aligned}$$

A 4 parameter fit gives

$$\begin{aligned} M_Z &= 91.188 \pm 0.013(\text{stat}) \pm 0.030(E_{\text{cm}})\text{GeV}/c^2 \\ \Gamma_Z &= 2.476 \pm 0.026(\text{stat}) \pm 0.010(\text{syst})\text{GeV}/c^2 \\ \Gamma_h &= 1.756 \pm 0.023(\text{stat}) \pm 0.020(\text{syst})\text{GeV}/c^2 \\ R &= 21.00 \pm 0.38(\text{stat}) \pm 0.29(\text{syst}). \end{aligned}$$

The corresponding values of the leptonic partial width (assuming lepton universality) and the invisible partial width are:

$$\begin{aligned} \Gamma_l &= 83.7 \pm 1.0(\text{stat}) \pm 1.1(\text{syst})\text{MeV}/c^2, \\ \Gamma_{\text{inv}} &= 469 \pm 19(\text{stat}) \pm 22(\text{syst})\text{MeV}/c^2. \end{aligned}$$

These values are also in good agreement with the standard model predictions:  $83.8 \pm 0.9\text{MeV}/c^2$  and  $502 \pm 5\text{MeV}/c^2$  respectively. In the minimal standard model the leptonic partial width can be expressed in terms of an effective weak mixing angle  $\sin^2(\overline{\theta}_W)$ . Using the measurement of  $\Gamma_l$  we find:

$$\sin^2(\overline{\theta}_W) = 0.2309 \pm 0.0048.$$

The number of light neutrino generations can be derived from  $\Gamma_{\text{inv}}$ :

$$N_\nu = 2.82 \pm 0.11(\text{stat}) \pm 0.13(\text{syst}).$$

With the values of the  $Z^0$  mass and total width fixed to the values obtained above the individual leptonic widths were obtained:

$$\begin{aligned} \Gamma_e &= 82.0 \pm 1.4(\text{stat}) \pm 1.3(\text{syst})\text{MeV}/c^2 \\ \Gamma_\mu &= 87.2 \pm 2.7(\text{stat}) \pm 2.2(\text{syst})\text{MeV}/c^2 \\ \Gamma_\tau &= 86.0 \pm 3.1(\text{stat}) \pm 2.7(\text{syst})\text{MeV}/c^2. \end{aligned}$$

Fixing the mass and width of the  $Z^0$  to the values given above, a one parameter fit to the "flavour-blind lepton" lineshape yields:

$$\begin{aligned} \Gamma_l &= 82.6 \pm 0.80(\text{stat}) \pm 0.80(\Gamma_Z) \\ &\quad 0.83(\text{lumi}) \pm 0.53(\text{syst})\text{MeV}/c^2. \end{aligned}$$

This is in good agreement with the result of the 4 parameter fit. The hadronic cross-section was compared to the standard model expectations via a fit in which only  $M_Z$  and an overall normalisation factor  $K$  were left free to vary. The results are:

$$\begin{aligned} M_Z &= 91.193 \pm 0.013(\text{stat}) \pm 0.030\text{GeV}/c^2 \\ K &= 1.019 \pm 0.005(\text{stat}). \end{aligned}$$

The quality of the fit [ $\chi^2/d.o.f = 13.1/(17-2)$ ] shows that the standard model with 3 neutrinos reproduces the data well. A 2 parameter fit to the tau and muon pair cross-sections and *forward-backward charge asymmetries* with  $M_Z$  and  $\Gamma_Z$  fixed to the above values, yields a measurement of the vector and axial-vector couplings of the  $Z^0$  to charged leptons (assuming universality). If we take the sign of these couplings to be negative, as determined by previous experiments, we obtain

$$\begin{aligned} v_l &= -0.111^{+0.049}_{-0.033}(\text{stat}) \pm 0.015(\text{syst}) \\ a_l &= -1.003 \pm 0.007(\text{stat}) \pm 0.01(\text{syst}). \end{aligned}$$

These results agree well with standard model expectations of -0.998 to -1.007 for the axial coupling and -0.056 to -0.095 for the vector coupling (by varying the top quark mass from 50 to 230

GeV and the Higgs mass from 30 to 1000 GeV). The results of this fits are displayed in Fig. 2.

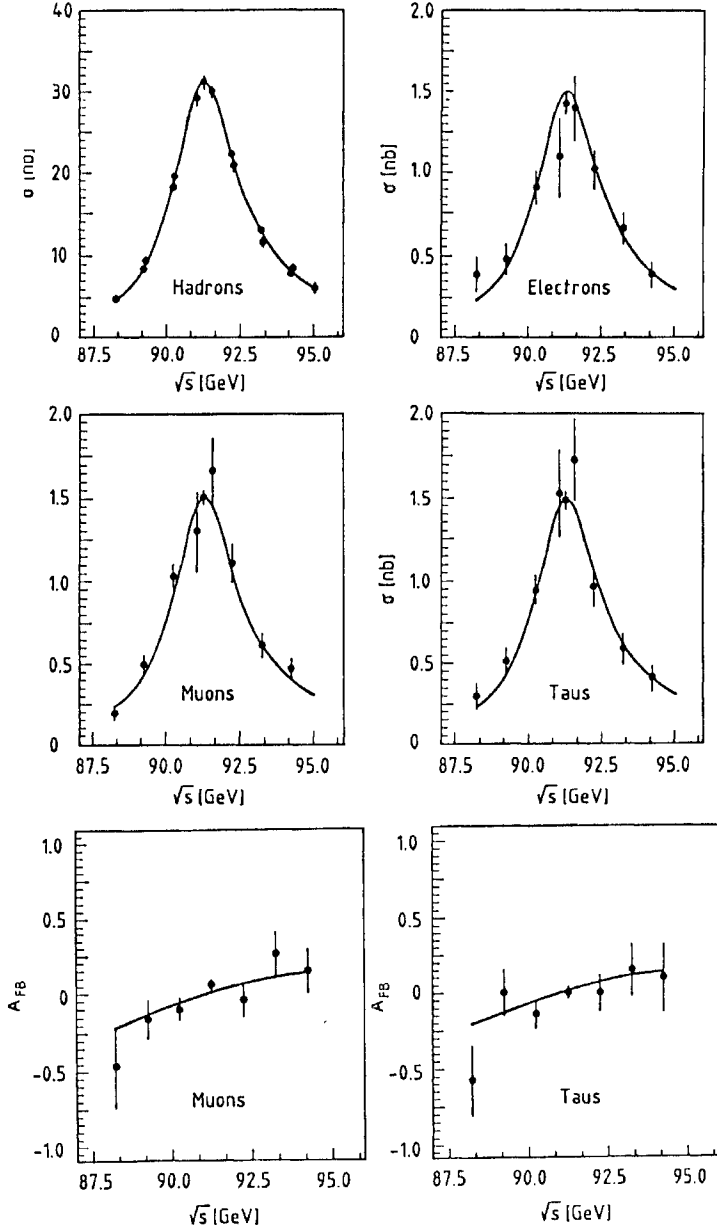


Figure 2 : Cross-sections of hadronic and leptonic decays of the Z-particle. The lower figures reproduce the forward-backward asymmetries in the muon- and tau- channels.

#### 4. Searches for new particles and decays.

In the searches described below samples of up to 70,000 events were used.

##### 4.1 Neutral standard higgsos.

Details of the search using the 1989 data have

been published [7]. The mass range  $210 \text{ MeV} \leq m_H \leq 14 \text{ GeV}/c^2$  was excluded (95% CL). An improvement in the upper limit has now been obtained from a study of the channels  $e^+e^- \rightarrow H^0 Z^*$  with  $Z^* \rightarrow e^+e^-, \mu^+\mu^-$  and  $\nu\bar{\nu}$ . For the charged leptonic channels a search was made for 2 high energy leptons (at least one with energy above 10 GeV), well isolated from the decay products of the Higgs. One  $e^+e^-H^0$  and no  $\mu^+\mu^-H^0$  candidates remain after the cuts. The  $e^+e^-$  candidate has a missing mass of about  $50 \text{ GeV}/c^2$ , and is outside the current range of sensitivity. For the channel  $\nu\bar{\nu}H^0$  the topology searched for was that of two misaligned jets, with a cut of  $\cos \xi$  of 0.8 in both the acoplanarity and acollinearity angles. The new upper limit is  $34 \text{ GeV}/c^2$ . A new search was performed for a very light Higgs boson, below the  $\mu\mu$  threshold. The search was conducted in two parts:

- a)  $0 \leq m_H \lesssim 60 \text{ MeV}$ . In this range there is a large probability that the  $H^0 \rightarrow ee$  or  $\gamma\gamma$  decay is outside the detector. The topology searched for was an acoplanar ( $> 5^\circ$ ) lepton-pair and nothing else.
- b)  $60 \lesssim m_H \leq 210 \text{ MeV}$ . In this range the  $H^0 \rightarrow ee$  decay would frequently be inside the fiducial region of the tracking chambers. A search was made for an isolated  $V^0$  with a lepton pair for the  $H^0 \ell^+ \ell^-$  ( $\ell = e, \mu$  or  $\tau$ ) channels. The  $V^0$  search algorithm was successfully tested by finding  $K^0$  and  $\Lambda^0$  decays in normal hadronic events (with mass resolutions of 20 MeV and 7 MeV FWHM respectively).

There were no candidates remaining after cuts in either a) or b). This excludes a light Higgs in the mass range from zero to 210 MeV at the 95% confidence level.

##### 4.2 Neutral higgsos in MSSM.

The results obtained with the 1989 sample data in the framework of the Minimal Supersymmetric Standard Model (MSSM) can be found in [8]. The new limits for  $m_h$  as a function of  $\tan \beta$  are shown in Fig. 3. Different methods, corresponding to different decay modes and different topologies, are used in the different domains of the plot. They are described in detail in a paper submit-

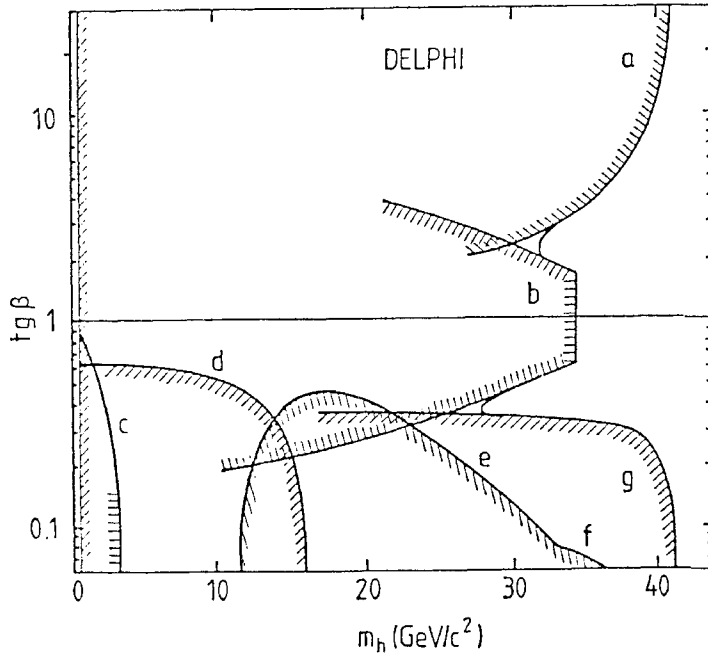


Figure 3 : Limits on the mass of the MSSM higgs  $h$ . The curves are explained in the text.

ted to the Conference [9]. The different curves in the plot correspond the following searches.

- a)  $\tau^+\tau^-$ +hadrons (mainly  $\tau^+\tau^- + b\bar{b}$ ). The method is to search for two isolated tracks (from  $\tau$  decays) accompanied by one or two jets. The 95% confidence level contour, taking into account the one candidate which survives the cuts, gives for  $m_h \approx m_A$  the limit  $m_h > 42 \text{ GeV}/c^2$ .
- b) This contour is obtained directly from the standard model search described in 4.1.
- c) This corresponds to the low mass domain where the decays are preferentially to pairs of  $\mu$ ,  $\pi$  or  $K$  [8].
- d) In this intermediate mass region the final state is mainly two hadronic jets. In  $hA$  events, unlike normal  $q\bar{q}$  events, there is no coloured string connecting the two jets and hence fewer particles are expected at wide angles from the jet axis.
- e) and f) correspond to searches in the 4-jet final state, the first one being based on inclusive charm tagging through  $D^{*\pm}$  production, the second on a global shape analysis [8].

- g) This contour corresponds to a new 4-jet analysis in which energy and momentum constraints are used to improve the mass resolution on heavy objects decaying into two hadronic jets.

In summary  $m_h > 28 \text{ GeV}$  for all values to  $tg\beta$ , while  $m_h \geq 32 \text{ GeV}$  for  $tg\beta > 0$ .

#### 4.3 Charged higgses.

Charged higgses can decay to either a pair of jets, mainly  $c\bar{s}$ , or to  $\tau\nu_\tau$ . The  $H^+H^-$  pair will therefore give rise to 4 jets, 2 prongs, or 2 jets-1 prong final states. The branching fraction into hadrons is treated as a free parameter, in order to produce model independent limits. The analyses concerning the 2 prong and the 2 jets-1 prong final states described in detail in [10] were applied to the 1990 data sample and no positive signal was obtained. For the 4-jets case, for the considered mass range (above  $30 \text{ GeV}/c^2$ ), the jet with the lowest energy was combined with the one with the highest energy. The resulting limits are [9]:

$$\begin{aligned} m_{H^\pm} &> 43 \text{ GeV}/c^2 \text{ for } Br(H^\pm \rightarrow \text{hadrons}) \simeq 0, \\ m_{H^\pm} &> 42 \text{ GeV}/c^2 \text{ for } Br(H^\pm \rightarrow \text{hadrons}) \simeq 0.5, \\ m_{H^\pm} &> 37 \text{ GeV}/c^2 \text{ for } Br(H^\pm \rightarrow \text{hadrons}) \simeq 1. \end{aligned}$$

#### 4.4 Squarks produced with non-interacting heavy stable particles.

We have recently [11] applied a new method to the search of heavy unstable charged particles which are pair created and decay immediately producing a neutral and non-interacting stable particle together with a standard quark. Decays of this type are to be expected in some theories beyond the Standard Model. Previous searches for these types of processes were based on the signature of a momentum imbalance appearing. Such approaches require a large difference between the masses. In the case of a *heavy* invisible object, close in mass to the decaying particle, the experimental signature changes from a clearly distinguishable acollinear jet topology to events of small visible energy.

The DELPHI search was based on two different analysis. The *first* one applies to heavy invis-

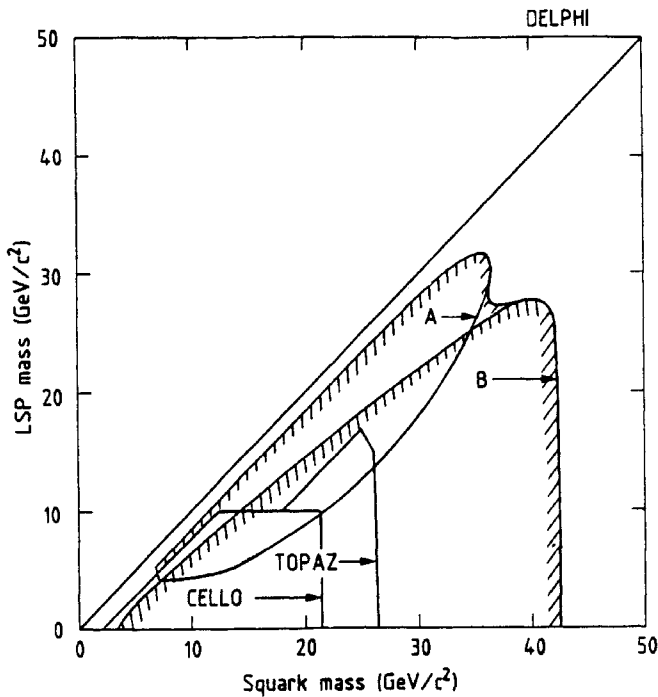


Figure 4 : Mass limits (95% C.L.) for non-degenerate up-squarks decaying into LSP's. The first and second method are labelled A and B.

ible objects and is new. It utilises  $e^+e^-$  annihilations at center-of-mass energies around the  $Z^0$  boson mass. The cross section of the new process is expected to follow the standard line shape of the  $Z^0$  boson and, thus, to exceed on the peak the cross section due to  $s$ -channel photon exchange by several orders of magnitude. Data points at center-of-mass energies around the  $Z^0$  pole are a direct experimental check of the estimates for the backgrounds which are decoupled from the  $Z^0$ . The *second* analysis was based on searching, as usual, for acollinear jets. The results of the search for up-squarks are compared in Fig. 4 with previous limits. Note how close to the  $45^\circ$  line the exclusion contour lies. Similar limits are obtained for down-squarks.

#### 4.5 Search for $Z \rightarrow \pi\gamma$ , and $\eta\gamma$ .

We have performed and submitted an analysis of the  $e^+e^-$  annihilation into two photons [12]. The main contribution to this reaction comes from a pure QED process, since the decay of the  $Z^0$  into two photons is forbidden by the Landau-Yang theorem. However, several allowed decays

of the  $Z^0$ , notably  $Z^0 \rightarrow \pi^0\gamma$  and  $Z^0 \rightarrow \eta\gamma$ , could lead to events with this topology. Through the analysis of the energy dependence of the cross-section, it is possible to identify the resonant contribution to this channel, and thus detect these decays.

Upper limits on  $Z^0$  decays into  $\pi^0\gamma$  and  $\eta\gamma$  can then be obtained by a likelihood analysis. We obtained the following limits at 95% confidence level :

$$\begin{aligned} \text{BR}(Z^0 \rightarrow \pi^0\gamma) &< (3.0 \times 10^{-4}) \\ \text{BR}(Z^0 \rightarrow \eta^0\gamma) &< (4.8 \times 10^{-4}). \end{aligned}$$

#### 4.6 Search for sleptons and charginos.

In the minimal supersymmetric scheme, one expects two charged and three neutral higgs boson particles. Accordingly there should be two pairs of charginos formed by mixing the weak eigenstates associated to W bosons (winos) and to charged higgs bosons (higgsinos). The lightest chargino pair is called  $\chi^\pm$ . The two heavy scalar particles, called sleptons, associated with the standard chiral leptonic states are denoted  $\tilde{\ell}_R^\pm$  and  $\tilde{\ell}_L^\pm$ . The  $\tilde{\ell}_R$  is expected to be the lightest but we have also tested the case of degenerate masses. Charginos and sleptons will decay into the lightest supersymmetric particle. The photino is assumed to be stable and to escape undetected since it has only weak interactions. A review of the production cross-sections for these particles, and of their decay properties, can be found in the previous DELPHI paper [13].

The events used to search for *unstable* sleptons and charginos correspond to about 40.000 hadronic  $Z^0$ 's. We required events with two oppositely charged tracks, both of them with a momentum higher than 2 GeV/c, at more than  $30^\circ$  with respect to the beam axis and with acoplanarity larger than  $15^\circ$ . As we have found no candidate for supersymmetric channels, we can derive limits in terms of  $m_{\tilde{\ell}}$  and  $m_\chi$  with two assumptions:

$$m_{\tilde{\ell}_R} = m_{\tilde{\ell}_L} \quad \text{or} \quad m_{\tilde{\ell}_L} \gg m_{\tilde{\ell}_R}.$$

We have determined the limits at 95% confidence level corresponding to the three slepton families [12]. These limits are above 44 GeV/c<sup>2</sup> for selectrons and smuons in the case of degenerate



masses, and above 43 GeV/c<sup>2</sup> if the masses are different. For staus the corresponding values are 42.5 and 40.5 GeV/c<sup>2</sup>. The coupling of the Z<sup>0</sup> to  $\chi^+\chi^-$  depends on the proportion of the wino and higgsino components. It is smallest for the case of pure higgsino. For the pure higgsino and pure gaugino cases we reach the kinematical limit.

If the lightest supersymmetric particle is not neutral, one could observe Z<sup>0</sup> 's decaying into two heavy *stable* charged particles. The final state is identified kinematically by looking for collinear two prongs where both measured momenta are equal and differ significantly from the beam momentum. For very high masses, close to the kinematical limit, the particles become non-relativistic. In this case the analysis of the momenta is not adequate. We have therefore searched for pairs of highly ionizing particles by looking for anomalous ionization in the TPC [12]. For stable sleptons, the absence of any candidate allows us to exclude the mass domain between 25 GeV/c<sup>2</sup> and 44.8 GeV/c<sup>2</sup> in the degenerate case, and up to 44.5 GeV/c<sup>2</sup> in the non-degenerate case. For stable charginos the limit is 45 GeV/c<sup>2</sup>.

## 5. Properties of hadronic events and QCD.

### 5.1 Multiplicity distributions and intermittency.

From a study of the multiplicity distributions we conclude that in the energy range 20-90 GeV approximate KN0 scaling is valid [14]. In particular the value of the dispersion  $D = 6.28 \pm 0.03 \pm 0.43$  of the distribution is equal to the one at lower energies. It was also shown that the Lund Parton Shower model describes the data reasonably well. The multiplicity distributions show positive forward-backward correlations that are strongest in the central region of rapidity and for particles of opposite charge. Later, we reached the same conclusion in [15], which is based on a data sample ten times larger.

Intermittency is a measure of the sporadic appearance of more hadrons in small volume of the available phase space. In the first paper on the subject, we have found that the relevant factorial moments in rapidity space are well described by the JETSET parton shower model [16]. This conclusion does not support the finding of the

TASSO collaboration [17]. Our later work, with much increased statistics, showed that the agreement is there also in 2-dimensional and 3-dimensional phase-space [18]. In conclusion, there is *no* need for physics beyond the one which is included in the best MC generators to explain the factorial moments of the multiplicity distributions at LEP energies.

### 5.2 Measurements of $\alpha_S$ .

DELPHI performed two independent measurements of the strong coupling constant by using the multijet rate [19] and the asymmetry of the energy-energy correlation [20]. The results are :

$$\alpha_S(91\text{GeV}) = 0.114 \pm 0.003(\text{stat}) \pm 0.004(\text{syst}) \pm 0.012(\text{th})$$

$$\alpha_S(91\text{GeV}) = 0.106 \pm 0.003(\text{stat}) \pm 0.003(\text{syst}) \begin{matrix} +0.003 \\ -0.000 \end{matrix} \text{th.}$$

The systematic errors are mainly due to hadronisation effects. The last error is due to the uncertainty in the choice of the renormalization scale. The asymmetry of the energy-energy correlation is much less sensitive to this choice [20] so that we can quote our best result on the QCD scale parameter :

$$\Lambda \frac{(5)}{\text{MS}} = \left[ 104 \begin{matrix} +20 \\ -20 \end{matrix} (\text{stat}) \begin{matrix} +25 \\ -20 \end{matrix} (\text{syst}) \begin{matrix} +30 \\ -0 \end{matrix} (\text{th}) \right] \text{MeV.}$$

### 5.3 Measurements of the triple gluon vertex.

DELPHI has submitted to the Conference the first measurement of a quantity which *measures* directly the triple gluon vertex. We have studied the bi-dimensional angular distributions of four jet events; previously only one-dimensional distribution had been used. Following R.K. Ellis et al [21], the transition probabilities to order  $\alpha_S^2$  can be grouped into gauge-invariant classes. For QCD the various probabilities are determined by the fermionic Casimir operation  $C_F=4/3$  and the number of colors  $N_C=3$ . By fitting the expected bi-dimensional distribution to the data we deduced [22]:

$$N_C/C_F = 2.05 \pm 0.4(\text{stat}) \begin{matrix} +0.7 \\ -0.1 \end{matrix} (\text{simul}) \pm 0.4(\text{frag}),$$

which is in agreement with the QCD expectation 2.25. Abelian theories would give  $N_C/C_F=0$ .

## 6. Partial widths in heavy flavours.

We have determined the partial width  $\Gamma_{c\bar{c}}$  of the  $Z^0$  boson into charm quark pairs, based on a total sample of 36 900  $Z^0$  hadronic decays [23]. The production rate of  $c\bar{c}$  events was derived from the inclusive analysis of charged pions coming from the decay of charmed meson  $D^{*+} \rightarrow D^0\pi^+$  and  $D^{*-} \rightarrow \bar{D}^0\pi^-$  where the  $\pi^\pm$  is constrained by kinematics to have a low  $p_T$  with respect to the jet axis. The probability to produce these  $\pi^\pm$  from  $D^{*\pm}$  decay in  $c\bar{c}$  events was taken to be  $0.31 \pm 0.05$  as measured at  $\sqrt{s} = 10.55$  GeV. The measured relative partial width

$$\Gamma_{c\bar{c}}/\Gamma_h = 0.162 \pm 0.030(\text{stat}) \pm 0.050(\text{syst})$$

is in good agreement with the Standard Model value of 0.171.

The  $b\bar{b}$  decay channel has a special event shape because of the high mass of the decaying particles. By using a technique based on a separation in boosted sphericity product, from a sample of  $Z^0$  events corresponding to an integrated luminosity of  $\sim 0.9 \text{ pb}^{-1}$  the fraction of  $b\bar{b}$  decays has been measured to be  $0.209 \pm 0.030(\text{stat}) \pm 0.031(\text{syst})$  [24]. The systematic error comes mainly from the uncertainty on  $b$  fragmentation function. Using our determination of the hadronic  $Z^0$  width, this corresponds to a partial width  $\Gamma_{b\bar{b}} = 367 \pm 76 \text{ MeV}$ , in good agreement with the Standard Model prediction of  $\simeq 380 \text{ MeV}$ .

## References

- [1] DELPHI Collaboration, P. Aarnio et al., CERN-PPE/90-128, Nucl. Instr. and Methods, in print.
- [2] DELPHI Collaboration, P. Abreu et al., CERN PPE/90-119, Submitted to the Singapore Conference, August 1990.
- [3] DELPHI Collaboration, P. Abreu et al., Phys. Lett. B231 (1989) 539, and B241 (1990) 435.
- [4] DELPHI Collaboration, P. Aarnio et al., Phys. Lett. B241 (1990) 425.
- [5] The ALIBABA program, W. Beenakker et al., University of Leiden, preprint (1990).
- [6] The ZFITTER/ZBIZON program package, D. Bardin et al., DELPHI 89-71 PHYS-52 (1989), D. Bardin et al., Zeit. Phys. C44 (1989) 493, and D. Bardin et al., Comp. Phys. Comm. 59 (1990) 303.
- [7] DELPHI Collaboration, P. Abreu et al., Nucl. Phys. B342 (1990) 1.
- [8] DELPHI Collaboration, P. Abreu et al., Phys. Lett. B245 (1990) 276.
- [9] DELPHI Collaboration, P. Abreu et al., CERN PPE/90-163, Submitted to the Singapore Conference, August 1990.
- [10] DELPHI Collaboration, P. Aarnio et al., Phys. Lett. B241 (1990) 449.
- [11] DELPHI Collaboration, P. Abreu et al., Phys. Lett. B247 (1990) 148.
- [12] DELPHI Collaboration, P. Abreu et al., CERN/PPE/90-167, Submitted to the Singapore Conference, August 1990.
- [13] DELPHI Collaboration, P. Abreu et al., Phys. Lett. B247 (1990) 157.
- [14] DELPHI Collaboration, P. Abreu et al., CERN/PPE/90-117, Submitted to the Singapore Conference, August 1990.
- [15] DELPHI Collaboration, P. Abreu et al., CERN/PPE/90-173, To be published in Zeitschrift für Physik C.
- [16] DELPHI Collaboration, P. Abreu et al., Phys. Lett. B247 (1990) 137.
- [17] TASSO Coll., Phys. Lett. B231 (1989) 548.
- [18] A. De Angelis, CERN-PPE/90-129 and Mod. Phys. Lett. A5 (1990) 2395.
- [19] DELPHI Collaboration, P. Abreu et al., Phys. Lett. B247 (1990) 167.
- [20] DELPHI Collaboration, P. Abreu et al., Phys. Lett. B252 (1990) 149.
- [21] R.K. Ellis et al., Nucl. Phys. B178 (1981) 421.
- [22] DELPHI Collaboration, P. Abreu et al., CERN/PPE/90-174, To be published in Phys. Lett. B.
- [23] DELPHI Collaboration, P. Abreu et al., Phys. Lett. B252 (1990) 140.
- [24] P. Abreu et al., CERN-PPE/90-118, Submitted to the Singapore Conference, August 1990.

# The First Year of OPAL on $Z^0$

T. Mori

*International Center for Elementary Particle Physics,  
Faculty of Science, University of Tokyo, Tokyo 113  
(The OPAL Collaboration)<sup>1</sup>*

## Abstract

Since its first observation of the  $Z^0$  at LEP last August, the OPAL detector has collected 112k hadronic decays and 11k leptonic decays of the  $Z^0$  at center-of-mass energies between  $-3\text{GeV}$  and  $+4\text{GeV}$  of the  $Z^0$  peak, by July, 1990. Based on measurements of total cross sections and forward-backward asymmetries of these decay modes, the mass of the  $Z^0$  boson, its total width, its partial widths into hadrons and leptons, and its invisible width (or the number of neutrinos) were determined in a model-independent way. The result was compared to the Standard Model predictions. In the framework of the Standard Model, the effective weak mixing angle was obtained from the data. Finally implication on the top quark mass was discussed.

## 1 OPAL

The OPAL Collaboration consists of about 300 physicists from 24 institutes in 9 different countries. The OPAL detector [1] is a general purpose detector situated at the CERN  $e^+e^-$  collider LEP. Trajectories of charged particles are measured by a jet chamber, a large volume drift chamber with 159 layers of wires in each of its 24 azimuthal sectors, together with a vertex detector and a  $z$ -chamber, with a momentum resolution of  $\Delta p/p = 10\%$  at  $p \approx 45\text{GeV}/c$ . Outside the tracking chambers is a solenoidal coil, a time-of-flight counter array, and an electromagnetic calorimeter, which measures electromagnetically showering particles with its 11,704 lead glass blocks and a pre-sampler, with an energy resolution of  $\Delta E/E = 3\%$  at  $E \approx 45\text{GeV}$ . An instrumented magnet return yoke serves as a hadron calorimeter, surrounded by four layers of outer muon chambers. Forward detectors measure the luminosity of LEP.

Here we report an improved measurement of the properties of the  $Z^0$  boson by the OPAL detector, based on a higher statistics data and smaller systematic errors than the previous publications [2,3,4]. The analysis presented here was based on the 123k  $Z^0$  events collected by July 25, 1990<sup>2</sup>.

## 2 Measurements of $Z^0$ Boson

Luminosity measurement by the forward

<sup>2</sup>The total number of events has increased  $\approx 50\%$  by the end of August, 1990.

calorimeter and the proportional tube chambers [3] has improved as the geometrical acceptance was better surveyed and the analysis and the calibration procedure were refined. Also, an independent measurement of the absolute luminosity by a set of scintillation counters became available. As a result, the systematic normalisation error has decreased to 1.6% and the fill-to-fill systematic error to 0.8%.

Hadronic decays of the  $Z^0$ , which have many charged and neutral hadrons in the final state, were selected by requiring a large number of energy clusters and a large energy deposit in the electromagnetic calorimeter. An acceptance of 97.7% was achieved with a background fraction of 0.4 – 0.5% due to  $\tau^+\tau^-$  events and two-photon multihadronic events. Selection based on charged tracks was also made, and agreement within better than 1% was observed. The systematic error was estimated to be 0.77%, which included the fragmentation uncertainty of 0.50%.

For the selection of leptonic decays of the  $Z^0$ , multihadronic events were efficiently rejected by requiring a low multiplicity in the event.

$e^+e^-$  decays of the  $Z^0$  were selected by identifying at least two high energy electromagnetic clusters associated with charged tracks. After the  $10^\circ$  acollinearity angle cut, the selection efficiency was found to be 99.5% within the angular acceptance of  $|\cos\theta_{e^-}| < 0.7$ , with a 1.0% systematic error.

Events were classified as  $\mu^+\mu^-$  candidates if they contained at least two muons, which were identified redundantly by the muon chamber, the hadron calorimeter, and the electromagnetic calorimeter. Cosmic ray events were rejected by time-of-flight measurements and track vertex re-

quirements. With a geometrical acceptance extended to  $|\cos\theta| < 0.95$ , the selection efficiency became 90.8% with an estimated systematic error of 0.9%.

$\tau^+\tau^-$  events were identified as events with two low-multiplicity jets of particles. While total energy cuts efficiently discriminated  $e^+e^-$  events, events accepted by the  $\mu^+\mu^-$  selection were rejected. With a  $15^\circ$  acollinearity cut between the jets and an acceptance cut of  $|\cos\theta| < 0.9$ , the selection efficiency of 73.9% was obtained. The total systematic error was estimated to be 1.9%.

For measurements of forward-backward asymmetries, leptonic decays in which both leptons were assigned the same charge were not used. Such events amounted to only 1.0-1.6% of the selected sample: the probability for double assignment of the wrong charge was thus negligible.

$b\bar{b}$  final states were extracted out of the hadronic sample by tagging decay leptons. The measured rate of such events, together with our measurement of the total hadronic width (see the following sections), was used to obtain the partial width of  $b$  quarks (Table 1). Forward-backward charge asymmetry of  $b\bar{b}$  events was also measured by using the charge of the tagged leptons. A more detailed account of this measurement can be found in [5].

Final state radiation in hadronic decays of the  $Z^0$  was first observed by our group [6]. Our measured total hadronic width, together with an updated measurement of final state radiation, allowed a determination of the partial widths of up and down type quarks [5]. The result was listed in Table 1.

The results of the measurements of cross sections and forward-backward asymmetries are shown in Figures 1-3, together with the previous measurements by the low energy experiments. They are also shown in Figures 5 and 6. Also indicated in Figure 1 was our measurement of the  $e^+e^- \rightarrow \gamma\gamma$  cross section.

### 3 Analysis

The uncertainties in the LEP energy scale were  $\pm 27$  MeV for the 1989 run and  $\pm 24$  MeV for the 1990 run. They were decomposed into a part fully correlated for the 1989 and the 1990 data ( $\pm 17$  MeV) and an additional uncorrelated part ( $\pm 21$  MeV and  $\pm 17$  MeV for 1989 and 1990 respectively).

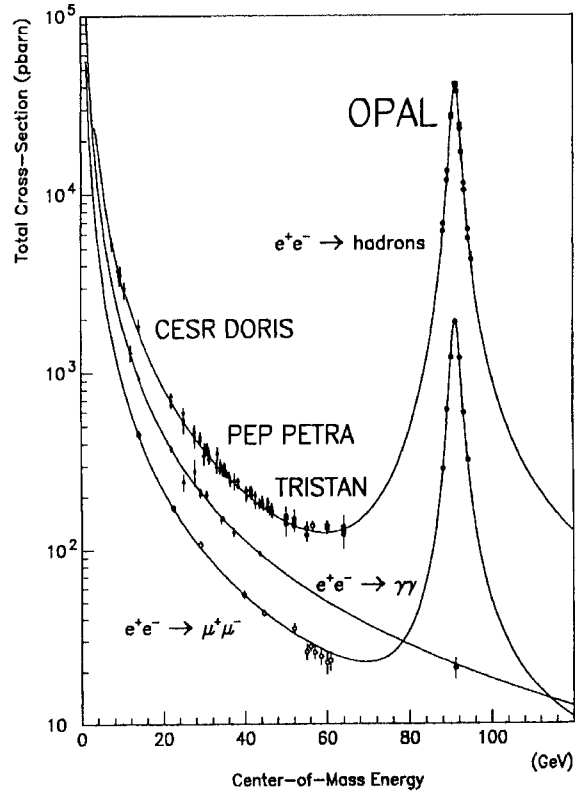


Figure 1: Cross section measurements of various  $e^+e^-$  processes.

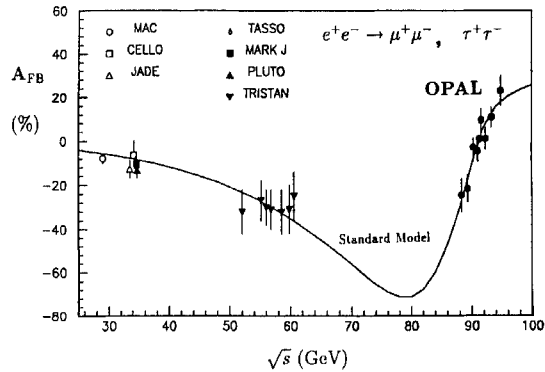


Figure 2: Forward-backward charge asymmetries for  $e^+e^- \rightarrow \mu^+\mu^-$  and/or  $\tau^+\tau^-$  processes.

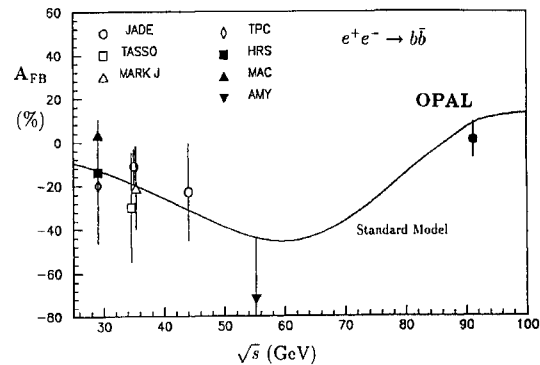


Figure 3: Forward-backward charge asymmetries for  $e^+e^- \rightarrow b\bar{b}$  processes.

These errors and their correlations were taken into account in the fits.

Radiative corrections significantly modify the cross sections and forward-backward asymmetries. For the calculation of the cross sections of  $q\bar{q}$ ,  $\mu^+\mu^-$ , and  $\tau^+\tau^-$  processes, the program ZFITTER [7] was used. Photonic corrections included in this program were a complete  $O(\alpha)$  calculation, leading  $O(\alpha^2)$ , and the exponentiation of soft photons. The calculated total cross sections agreed with that obtained from the program ZSHAPE [8] to better than 0.2 %. The effects of cuts on the differential cross section reproduced the results obtained with the KORALZ program [9] to better than 0.5 % over the energy range of interest.

The presence of  $t$ -channel exchange diagrams in the  $e^+e^- \rightarrow e^+e^-(\gamma)$  process, which were not included in the ZFITTER calculation, complicates the treatment of this process. Recently a new calculation for this process has become available in the form of the program ALIBABA [10]. It included contributions from lowest order and all one-loop and box diagrams. Photonic corrections were treated exactly to first order with a leading log summation for higher order terms. The ALIBABA program was unfortunately too slow to be used in the fits. Therefore we used it to calculate the contributions of the  $t$ -channel exchange and  $s$ - $t$  interference terms for the  $e^+e^-$  process, and they were subtracted from the measured cross sections and asymmetries (" $t$ -channel subtraction"). The resulting cross sections and asymmetries were then considered as a pure  $s$ -channel process, and the ZFITTER was used to fit them.

As a check to the ALIBABA calculation, the  $t$ -channel subtraction procedure was repeated for different angular ranges and the fit results were compared; the observed changes were consistent with statistical fluctuations. We assigned a 5 % systematic error to the  $t$ -channel subtraction, inflated from the 0.5 % uncertainty quoted in [10], which is still negligible compared to the current statistical errors.

### 3.1 Hadronic Line Shape

A model independent fit with the mass  $M_Z$ , the width  $\Gamma_{Z^0}$ , and the peak cross section  $\sigma_{had}^{pole}$  was performed to the hadronic cross sections. The result was  $M_Z = 91.164 \pm 0.011 \pm 0.021 \text{ GeV}/c^2$ ,  $\Gamma_{Z^0} = 2.496 \pm 0.021 \text{ GeV}$ , and  $\sigma_{had}^{pole} = 41.88 \pm 0.74 \text{ nb}$  with  $\chi^2/ndf = 8.9/13$ . The second error on  $M_Z$  was due to the LEP beam energy uncertainty.

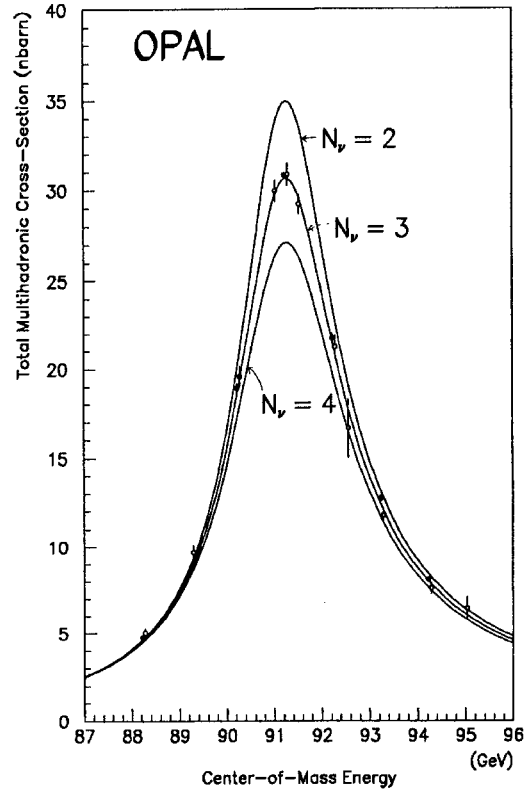


Figure 4: Hadronic line shape compared with the Standard Model predictions for  $N_\nu = 2, 3, 4$ .

Figure 4 compares our result with the Standard Model predictions; it was totally compatible with the Standard Model with the number of light neutrinos  $N_\nu = 3$ , and the possibility of  $N_\nu = 2$  or 4 looked completely abandoned.

### 3.2 Leptonic Data – Combined Fits

Both the cross sections and the charged asymmetries of the leptonic decays were used to extract the partial widths of the  $Z^0$  boson. In all of the following fits, if not explicitly mentioned, the hadronic cross sections were also used in order to account properly for the correlated errors with  $M_Z$ ,  $\Gamma_{Z^0}$ , and the hadronic partial width,  $\Gamma_{had}$ , which were also treated as free parameters in the fits.

The differential cross section for  $s$ -channel fermion-pair production can be expressed as:

$$\frac{d\sigma}{dc} \propto (C_{\gamma\gamma} + C_{ZZ}|\chi|^2)(1+c^2) + (A_{ZZ}|\chi|^2 + A_{\gamma Z} \text{Re}\chi)c$$

where  $c = \cos\theta$  and  $\chi \propto s/(s - M_Z^2 + is\Gamma_{Z^0}/M_Z)$ . Here only the dominant terms were indicated. The most dominant  $C_{ZZ}$  determines the total cross sections. While the forward-backward asymmetry at the  $Z^0$  resonance is determined by  $A_{ZZ}/C_{ZZ}$ , the

ratio  $A_{\gamma Z} Re\chi/(C_{ZZ}|\chi|^2)$  describes the energy evolution of the asymmetry. These coefficients are simply related to the vector and axial vector couplings of the  $Z^0$  to the fermion at tree level. Higher order corrections, however, modify this relationship in a model-dependent way. We used our measurements of leptonic final states to determine these coefficients without any presumed relation-

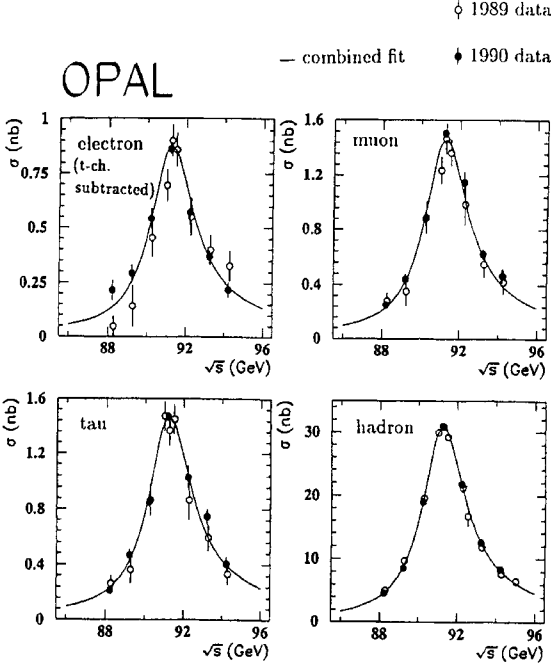


Figure 5: Cross sections for various decays of the  $Z^0$ . Drawn are the combined fit result.

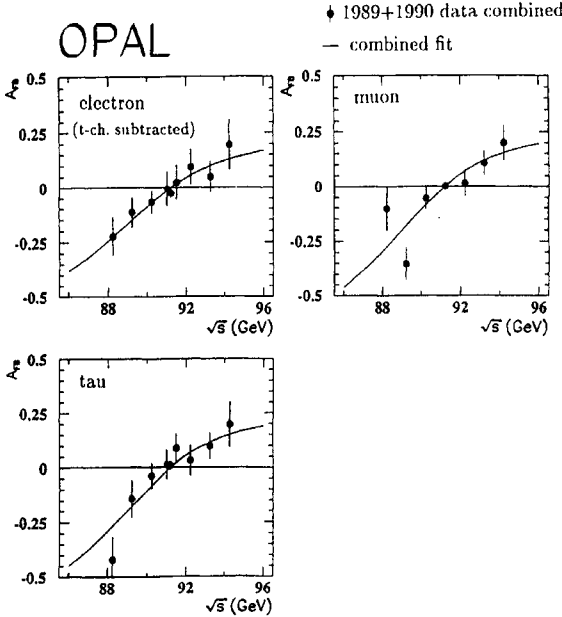


Figure 6: Forward-backward charge asymmetries of leptonic decays of the  $Z^0$ . Drawn are the combined fit result.

ship among them. In the fit, we parametrized the coefficients in terms of the effective leptonic coupling constants,  $\hat{a}_l^2 v_l^2$  and  $\hat{a}_l^2$ , and the partial widths of the leptons,  $\Gamma_{l+l-}$ , in the following way:

$$C_{ZZ} \propto \Gamma_{l+l-}^2, \quad A_{ZZ} \propto \hat{a}_l^2 v_l^2, \quad A_{\gamma Z} \propto \hat{a}_l^2,$$

and they were treated as completely independent. The fit resulted in  $\Gamma_{e^+e^-} = 82.7 \pm 1.3$  MeV,  $\Gamma_{\mu^+\mu^-} = 85.9 \pm 2.0$  MeV,  $\Gamma_{\tau^+\tau^-} = 83.9 \pm 2.3$  MeV,  $\hat{a}_l^2 v_l^2 = 0.0036 \pm 0.0034$ , and  $\hat{a}_l^2 = 0.98 \pm 0.13$ , with  $\chi^2/ndf = 68.4/83$ , fully consistent with the principle of lepton universality, and also with the Standard Model prediction.

With the assumption of lepton universality, the fit yielded  $\Gamma_{l+l-} = 83.6 \pm 1.0$  MeV with  $\chi^2/ndf = 70.2/86$ . At the same time,  $M_Z = 91.174 \pm 0.011$  GeV/ $c^2$ ,  $\Gamma_{Z^0} = 2.505 \pm 0.020$  GeV, and  $\Gamma_{had} = 1.778 \pm 0.026$  GeV were obtained from the fit. The curves drawn in Figures 1, 2, 5, and 6 were the fit result. It is evident from the figures that the fit result described the whole spectrum of the  $e^+e^-$  reaction pretty well. In fact, it described not only the line shapes and the asymmetries but also the differential cross sections as well (Figure 7).

The same fit also gave a model-independent determination of the invisible width of the  $Z^0$ ,  $\Gamma_{inv}$ , to be  $476 \pm 25$  MeV, and the number of the light neutrino species (or the number of generations),  $N_\nu \equiv \Gamma_{inv}/\Gamma_\nu$ , to be  $2.86 \pm 0.15_{-0.04}^{+0.02}$ , where the second errors came from the uncertainties in  $m_{top}$ ,  $m_H$ , and  $\alpha_S$  ( $m_{top} = 50 - 250$  GeV/ $c^2$ ,  $m_H = 20 - 1000$  GeV/ $c^2$ ,  $\alpha_S = 0.09 - 0.15$ ). The ratio of the hadronic and the leptonic partial widths was  $R_Z \equiv \Gamma_{had}/\Gamma_{l+l-} = 21.26 \pm 0.32$ , which should be compared to the Standard Model prediction of  $20.6 - 21.1$  where the uncertainties in  $m_{top}$ ,  $m_H$ , and  $\alpha_S$  were taken into account.

The differential cross section can be also expressed directly in terms of  $\hat{a}_l^2$  and  $v_l^2$  in the form of the improved Born approximation [11], in which the tree level relationship among the coefficients,  $C_{ZZ}$ ,  $A_{ZZ}$ , and  $A_{\gamma Z}$ , was assumed (i.e.,  $\Gamma_{l+l-} \propto \hat{a}_l^2 + v_l^2$  etc.). A fit using this parametrization yielded a very precise determination of the couplings:  $\hat{a}_l^2 = 1.005 \pm 0.012$  and  $v_l^2 = 0.0038 \pm 0.0033$  with  $\chi^2/ndf = 70.2/86$ , in a good agreement with other measurements [12].

The effective couplings may be written in terms of  $\rho_Z$  and the effective weak mixing angle  $\sin^2 \bar{\theta}_W$  by

$$\hat{a}_l^2 \rightarrow \rho_Z, \quad v_l^2 \rightarrow \rho_Z(1 - 4 \sin^2 \bar{\theta}_W)^2.$$

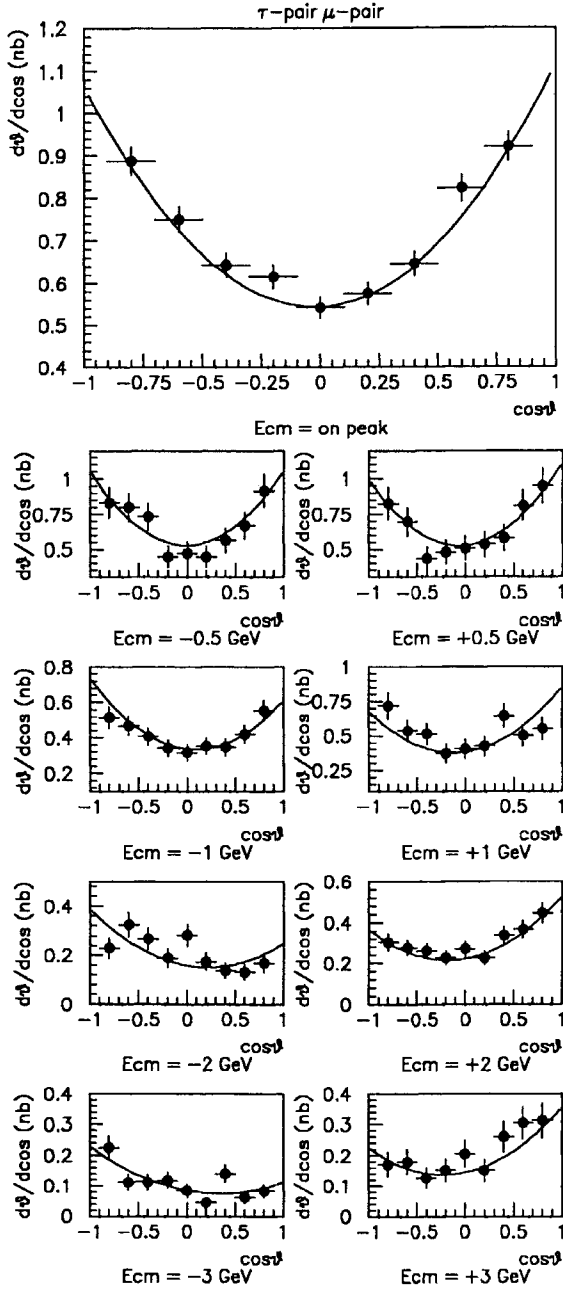


Figure 7: Differential cross sections of  $e^+e^- \rightarrow \mu^+\mu^-, \tau^+\tau^-$ . Drawn are the combined fit result.

In this parametrization, the  $\rho_Z$  parameter mainly determines the total cross section while  $\sin^2 \bar{\theta}_W$  describes the asymmetry. A fit treating  $\rho_Z$  and  $\sin^2 \bar{\theta}_W$  as independent parameters yielded  $\rho_Z = 1.005 \pm 0.012$  and  $\sin^2 \bar{\theta}_W = 0.2316^{+0.0095}_{-0.0057}$  as shown in Figure 8, if the  $\chi^2$  minimum for  $\sin^2 \bar{\theta}_W < 0.25$  was chosen. With the minimal Standard Model relationship between  $\rho_Z$  and  $\sin^2 \bar{\theta}_W$  imposed (indicated as a line in Figure 8), the fit resulted in a more precise determination of the effective weak mixing angle,  $\sin^2 \bar{\theta}_W = 0.2315 \pm 0.0028$ .

### 3.3 Top Quark Mass

Within the framework of the minimal Standard Model, our data were used to constrain the top quark mass,  $m_{top}$ .

A fit to the OPAL measurements of the line shapes and the asymmetries resulted in the central value of  $m_{top} = 154 \text{ GeV}/c^2$ . On the other hand, if our measured value of  $M_Z$  was used together with the  $M_W/M_Z$  values measured by the UA2 and the CDF experiments,  $m_{top} = 143 \text{ GeV}/c^2$  was obtained. Both values, which could be considered as independent estimates of  $m_{top}$ , coincided within  $\approx 10 \text{ GeV}/c^2$ , strongly suggesting that  $m_{top}$  lie around that region.

By combining our measurements of line shapes and asymmetries and the  $M_W/M_Z$  measurements, we obtained  $m_{top} = 144^{+59}_{-50} \text{ GeV}/c^2$ , where uncertainties in  $\alpha_S$  of  $\pm 0.02$  and in  $m_H$  of  $40 - 1000 \text{ GeV}/c^2$  were taken into account.

## 4 Summary

We measured the cross sections and the forward-backward charge asymmetries of various  $Z^0$  decays with the OPAL detector. Using these measurements, we determined the properties of the  $Z^0$ , such as the mass, the width, and the couplings to the various fermions (Table 1). Their agree-

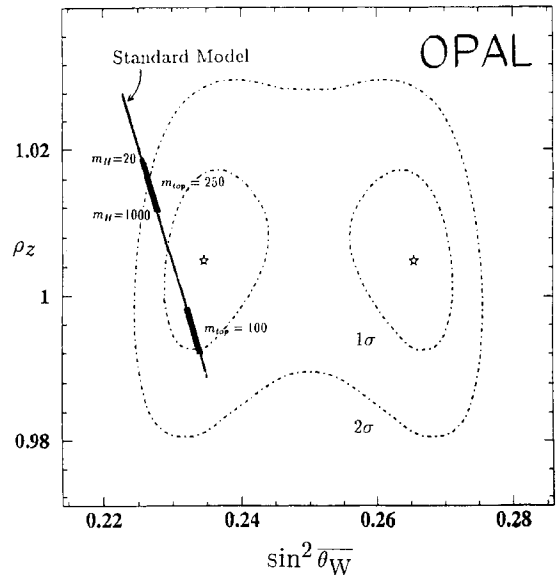


Figure 8: Confidence level contour plot of the  $\sin^2 \bar{\theta}_W$  fits. The stars indicate the best fit points. The line shows the minimal Standard Model prediction.

ments with the Standard Model predictions were impressive. Our model-independent determination of the invisible width of the  $Z^0$  constrained the number of generations to be  $2.86 \pm 0.15$ .

In the context of the minimal Standard Model, the weak mixing angle,  $\sin^2 \theta_W$ , was determined to be  $0.2315 \pm 0.0028$ . The top quark mass evaluated from our data agreed with that obtained from the  $M_W/M_Z$  measurements at the  $\bar{p}p$  colliders and our  $M_Z$  value, indicating  $m_{top}$  be as high as  $\approx 150 \text{ GeV}/c^2$ . Finally, combining our data and the  $M_W/M_Z$  measurements yielded  $m_{top} = 144_{-50}^{+59} \text{ GeV}/c^2$ .

## 5 Acknowledgements

We would like to thank the conference organisers for their hospitality. It is a pleasure to thank CERN SL Division for the smooth operation of the LEP accelerator, precise information on the absolute energy, and their continuing close cooperation with our experimental group. In addition to the support staff at the collaborating institutions, we are pleased to acknowledge: Department of Energy, USA, National Science Foundation, USA, Science and Engineering Research Council, UK, Natural Sciences and Engineering Research Council, Canada, Israeli Ministry of Science, Min-

$M_Z$	$91.174 \pm 0.011 \pm 0.021 \text{ (GeV}/c^2\text{)}$
$\sigma_{had}^{pole}$	$41.88 \pm 0.74 \text{ (nb)}$
$\Gamma_Z$	$2.505 \pm 0.020 \text{ (GeV)}$
$\Gamma_{had}$	$1.778 \pm 0.026 \text{ (GeV)}$
$\Gamma_{ee}$	$82.7 \pm 1.3 \text{ (MeV)}$
$\Gamma_{\mu\mu}$	$85.9 \pm 2.0 \text{ (MeV)}$
$\Gamma_{\tau\tau}$	$83.9 \pm 2.3 \text{ (MeV)}$
$\Gamma_{l+l-}$	$83.6 \pm 1.0 \text{ (MeV)}$
$\Gamma_{inv}$	$476 \pm 25 \text{ (MeV)}$
$(N_\nu)$	$(2.86 \pm 0.15)$
$\hat{a}_1^2$	$1.005 \pm 0.012$
$\hat{v}_1^2$	$0.0038 \pm 0.0033$
$\Gamma_{up}$	$330 \pm 99 \text{ (MeV)}$
$\Gamma_{down}$	$369 \pm 67 \text{ (MeV)}$
$\Gamma_{bb}$	$363 \pm 47 \text{ (MeV)}$
$\sin^2 \theta_W$	$0.2346_{-0.0057}^{+0.0095}$
$\rho_Z$	$1.005 \pm 0.012$
$\sin^2 \theta_W$	$0.2315 \pm 0.0028$
$m_{top}$	$144_{-50}^{+59} \text{ (GeV}/c^2\text{)}$

Table 1: A summary of OPAL results. 123k  $Z^0$  events collected by July 25, 1990 were used in the analysis. The second error of  $M_Z$  was due to the LEP energy uncertainty.

erva Gesellschaft, The Japanese Ministry of Education, Science and Culture (the Monbusho) and a grant under the Monbusho International Science Research Program, American Israeli Bi-national Science Foundation, Direction des Sciences de la Matière du Commissariat à l'Énergie Atomique, France, The Bundesministerium für Forschung und Technologie, FRG, and the A.P Sloan Foundation.

## References

- [1] *The OPAL Detector at LEP*, OPAL Collab., CERN-PPE/90-114 (1990), to be published in Nucl. Instr. and Meth.
- [2] OPAL Collab., Phys. Lett. B231 (1989) 530.
- [3] OPAL Collab., Phys. Lett. B240 (1990) 497.
- [4] OPAL Collab., Phys. Lett. B235 (1990) 379.
- [5] A. Jawahery (OPAL Collab.), presented in this conference.
- [6] OPAL Collab., Phys. Lett. B246 (1990) 285.
- [7] D.Yu. Bardin et al., Berlin-Zeuthen preprint, PHE 89-19 (1989); Z Physics at LEP 1, CERN 89-08, ed. G. Altarelli et al., Vol 3 (1989) 60.
- [8] W.J.P. Beenakker, F.A. Berends and S.C. van der Marck, Institut-Lorentz, Univ. Leiden; Z Physics at LEP 1, CERN 89-08, ed. G. Altarelli et al., Vol 3 (1989) 50.
- [9] S. Jadach et al.; Z Physics at LEP 1, CERN 89-08, ed. G. Altarelli et al., Vol 3 (1989) 69.
- [10] W.J.P. Beenakker, F.A. Berends and S.C. van der Marck, Institut-Lorentz, Univ. Leiden, preprint, "Large Angle Bhabha Scattering at LEP" (1990).
- [11] M. Consoli and W. Hollik, Z Physics at LEP 1, CERN 89-08, ed. G. Altarelli et al., Vol 1 (1989) 7.
- [12] U. Amaldi et al., Phys. Rev. D36 (1987) 1385; G. Costa et al., Nucl. Phys. B297 (1988) 244; G.L. Fogli and D. Haidt, Z. Phys. C40 (1988) 379; CHARM Collab., Z. Phys. C41 (1989) 567; K. Abe et al., Phys. Rev. Lett. 62 (1989) 1709; CHARM II Collab., Phys. Lett. B232 (1989) 539.